UNDERSTANDING SCALP EEG IN RESPONSE TO NEWSVENDOR DECISION-MAKING AND FEEDBACK

by

MOBASSHIR HOSSAIN AKASH

Presented to the Faculty of the Graduate School of

The University of Texas at Arlington in Partial Fulfillment

of the Requirements

for the Degree of

MASTER OF SCIENCE IN BIOMEDICAL ENGINEERING

THE UNIVERSITY OF TEXAS AT ARLINGTON

MAY 2019

Acknowledgements

I would like to thank the Almighty Allah for being my strength, helper, and sufficiency throughout the period of my Master's program. Then, my deepest appreciation goes to my mentor and supervisor, Dr. Hanli Liu, for her patience, support, and persistent guidance throughout the duration of my research work. Her immense knowledge, ways of teaching, effective approach towards research work, and effective suggestions have made a huge impact on me, which would definitely help me on my future endeavors. I would like to greatly appreciate Dr. Kay Chen and Dr. Sridhar Nerur for helping me better understanding their protocol, and also for their collaboration in this project. Also, I would like to thank them for accepting the invitation to be in my defense committee.

Firstly, my thanks go to Hashini Wanniarachchi, who was my partner in collecting the EEG data used for this study. Also, I greatly appreciate Yan lang for his time during data collection, and Gauri Kathote, who helped me during data collection, and data processing. In addition, I also thank Dr. Xinlong Wang for giving his ideas of better showcasing, and helping me with interpretation of data. I would like to appreciate other members of Dr. Liu's lab, who volunteered themselves as subjects for my study.

My sincere thanks also go to my loving parents, Mr. Mohammad Hossain Bhuiyan, and Ms. Fathema Johora Nilu, for their moral support and unconditional love throughout this journey. Last but not the least, I got some valuable friends during this journey, who were there to support me during my good and bad times. I would like to thank all of them, specially- Athena, Yudhajit, Rafi, Sanju, Arnila, Ola, and Zaid.

April 25, 2019

Abstract

Understanding scalp EEG in response to newsvendor decision-making and feedback

Mobasshir Hossain Akash, MS

The University of Texas at Arlington, 2019

Supervising Professor: Dr. Hanli Liu

Abstract:

Neuroeconomics is an emerging field integrating economic theories with neuroscience to enhance the understanding on how humans make decisions under different cost-effective conditions. Understanding the brain network associated with different cognitive tasks, to investigate the basic neural processes that underlie complex higher-order cognitive operations, has become an important research topic in behavioral neuroscience. Newsvendor problem plays a vital role among all prevalent concepts. This study is designed based on Newsvendor problem incorporating 40 trials for each subject at a randomly chosen low-profit or high-profit margin treatments to investigate how electrophysiological signals in the human brain are differentiated under the two treatments using 64-channel electroencephalography. The electrophysiological data were collected from 13 subjects while they were making decisions under randomly assigned two treatment levels with a MATLAB-based newsvendor game. Power density analysis of EEG signals was performed in 5 frequency components of EEG, which were delta (1–4 Hz), theta (4 –8 Hz), alpha (8–13 Hz), beta (13–30 Hz), and gamma (30–70 Hz) for three experimental phases, namely: baseline, decision

making, and feedback. Root-Mean-Square (RMS) values of power calculation from each frequency band of each electrode was calculated using MATLAB; then 64-channel RMS magnitudes were averaged over all the participants to generate group-level topographical maps for all five frequency bands and throughout the three different phases.

The group-level topographies across all five bands show significant activations in several major scalp regions during high- and low-margin task phases. Paired-sample t-tests with false-discovery-rate correction ($p<0.05$) were conducted to identify significant electrodes across different treatments for multi-variable comparisons. Five clusters were identified from the 64-channel scalp region based on the common electrodes that shows statistical significance in one of the frequency bands. The cluster-based analysis indicated that significant activation by the newsvendor decision making occurred in the dorsolateral prefrontal cortex at four brain rhythm bands, excluding the gamma frequency. Also, power densities in alpha and theta bands shows opposite activation trends during the decision-making and feedback phase. Previous studies reported that the theta band plays a key role in memory retrieval and decision making. Our findings showed that the theta activation was significantly observed in all five clusters during the newsvendor decision-making phase. On the other hand, this specific decision making did not cause any change in beta band power. However, after splitting these data into low- and high-margin treatment conditions, it showed significant deactivation in the right dorsolateral prefrontal cortex during the decision-making phase under the low-margin treatment, reflecting mental stress or anxiety, as expected.

Table of Contents

LIST OF ILLUSTRATIONS

LIST OF TABLES

CHAPTER 1
INTRODUCTION

1.1 **Newsvendor Problem:**

Neuroeconomics is gaining momentum in the interdisciplinary studies involving economics and neuroscience. Behavioral studies of models for managing inventory in the face of demand uncertainty have received significant attention in the literature in the past decade (e.g., Schweitzer & Cachon, **2000**;) [1]. Among all the prevalent concepts, Newsvendor Problem plays the most vital role.

Newsvendor Problem (NP) is an attractive economic decision-making scenario which is associated with single-term estimation of determining the order quantity which maximizes the expected profit (or minimizes the expected loss) in a single period probabilistic demand framework [2]. Newsvendor problem or single-period problem (SPP) plays a key role at the conceptual foundations of stochastic inventory theory, which is related to decision-making under stochastic uncertainty or risk, where the demand is from a known probability distribution. The traditional concept of this problem is that the decision-maker (e.g. storekeeper or manager), who retails a merchandise facing uncertainty demand distribution, has to decide how many units to buy each day without storing excess inventory [3].

The newsvendor problem was first presented by Whitin (1955), since then it has become one of the classic models in inventory management. This problem primarily focuses on the purchase of perishable products. The mathematical model maximizes the expected profit by determining the optimal order-size. For the sake of convenience, the order-size of the maximal expected profit is

abbreviated as 'Optimal order'. Optimal order and expected profit are functions of: (1) the item cost and the marginal profit, and (2) the demand distribution

In a decision contained risk, the likelihood of the consequence is known. However, the safe or risky outcome differs in terms of the reward[4]. Newspaper vendors, milk sellers are examples of real-life applications of this scenario to determine their daily order quantity.

1.2 Economic Decision Making Using EEG:

Carlson and O'keefe (1969) were the first to report an experiment with the newsvendor problem. In that context, NP was part of a much larger experiment in scheduling decision-making. No specific conclusions could have been made from that experiment other than an analogy. Other researchers used different context or phenomenon to indicate order-purchase decisions correspond to the optimal order, but not any of them are designed to disentangle biases in the newsvendor context. Cachon and Schweitzer (2000) used the newsvendor problem to conduct an important experimental test [5]. They analyzed 15 decision periods of ordering for each subject with known uniform distribution. Their experimental study showed that participants tend to order less than the optimal order, when the marginal profit is larger than the cost, indicating a deviation from the optimal order. Bolton (2004) used 100 decision rounds and found that enhanced experience improves newsvendor performance, even though this improvement is on average, pretty slow.

Here, in our case, we conducted an experimental study using the newsvendor problem for 40 decision making rounds to indicate the optimal decision making progress of a human subject. Using a brain imaging modality will help us to identify which part of the brain is simultaneously getting activated or deactivated during this complex decision making process. Also, profit/loss

has a huge impact in emotional behavior, which certainly can lead us to different behavioral response in the brain related to reward processing. To best of our knowledge, not many of the studies have been conducted from a behavioral perspective in the simple newsvendor setting.

There are several brain imaging modalities such as functional magnetic resonance imaging (fMRI), functional near-infrared spectroscopy (f-NIRS), and electroencephalography (EEG). EEG is a widely used non-invasive optical imaging technique which has the ability to measure neural activity based on electrical signals in the brain directly. Moreover, EEG can detect neurophysiological activity during different tasks and conditions in millisecond precision. Even though EEG has a very high temporal resolution compared to fMRI and fNIRS, it is inexpensive, easy-to-use under simple conditions and portable neuroimaging modality. To examine the neuroeconomics behind the newsvendor problem, we incorporated a computer game-based platform with EEG modality to understand the neurophysiological functions. Many studies have been reported EEG as a noninvasive robust optical imaging tool for decision-making research [37] [38].

1.3 Motivation of this study:

Understanding human thought and behavior can take many approaches, but to really understand how the brain works, one may need to look deep inside it. As many brain imaging methods today are entirely noninvasive, it shouldn't be difficult to track the brain response corresponds to different neural activity. The purpose of the study is to examine how brain activates during complex decision-making task with multiple conditions. Previous literature reported that there are three foremost neural networks play roles in the process. They are namely, reward processing, cognitive control, and social cognition. These processes trigger mainly dorsolateral

prefrontal cortex (DLPFC), orbitofrontal cortex (OFC) and angular cingulate cortex (ACC) along with several other regions in the brain as a network as shown in the fMRI studies [6]. However, we hypothesized that dorsolateral prefrontal cortex (DLPFC) which represents cognitive control, and orbitofrontal cortex (OFC), which is a part of reward pathway, are the major brain areas were to activate during a decision-making task at the cortical level using our fNIRS study. This study focuses on making economic-decisions of weighing gains and losses under risk and uncertain demand distribution, and to detect the changes of electrophysiological activity in the brain during this decision-making process, we have incorporated a robust imaging modality called, Electroencephalography (EEG).

1.4 What is EEG?

EEG (electroencephalography) measures the electrical activity of the brain placing electrodes on our scalp level. It tells us how active the brain is, from the surface measurements. Measuring electrical activity reflects how the many different neurons in the brain network communicate with each other via electrical impulses. This can be useful for quickly determining how brain activity can change in response to stimuli, and can also be useful for measuring abnormal activity, such as with epilepsy.

Several reasons why we are incorporating EEG as a functional imaging tool for our decision-making research.

- ✓ EEG has very high time resolution and captures cognitive processes in the time frame in which cognition occurs.
- ✓ EEG directly measures neural activity.
- ✓ EEG is inexpensive, lightweight, and portable.

✓ EEG monitors cognitive-affective processing in absence of behavioral responses.

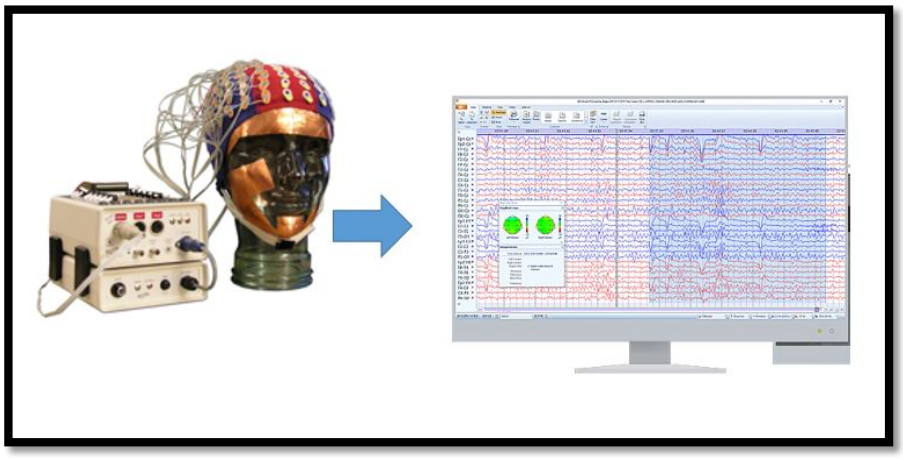

Figure 1.1: A schematic presentation of regular EEG experiment, using head-cap, electrodes, USB converter, recording device and computer to display the recordings. (Reference: https://electronics.stackexchange.com/questions/413727/what-device-can-convert-eeg-voltage-data-to-real-voltage)

1.4.1 EEG Rhythms and Oscillations:

Understanding different brain oscillations recorded by EEG rhythms are the key features of studying the neurophysiological functions in response to the news-vendor based decision-making research. Primarily EEG has 5 main rhythms, namely- Delta, Theta, Alpha, Beta, Gamma. Each of these rhythms have different physiological functions corresponding to the brain stimuli.

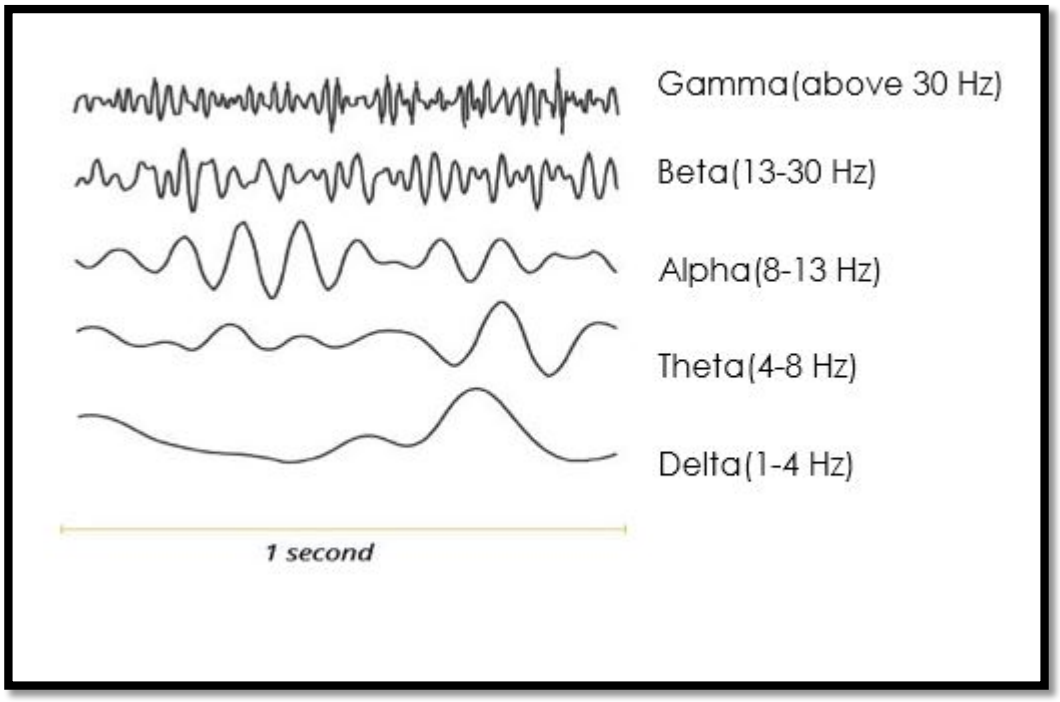

Figure 1.2: Different EEG rhythms and oscillations (Reference: https://imotions.com/blog/eeg/)

Delta Band (1-4 Hz):

"Delta waves are characterized as the slowest and highest amplitude brainwaves, oscillations ranging in between 1 – 4 Hz (Niedermeyer & da Silva, 2012). These waves are only present during deep non-REM sleep (stage 3), also known as slow-wave sleep (SWS). In sleep labs, delta waves are examined to assess the depth of sleep. The stronger the delta rhythm, the deeper the sleep. Increased delta power (an increased quantity of delta wave recordings) has also been found to be associated with increased concentration on internal working memory tasks" [8] [9].

Theta Band (4-8 Hz):

"Brain oscillations within the 4 – 8 Hz frequency range are referred to as theta band (Niedermeyer & da Silva, 2012). Studies consistently report frontal theta activity to correlate

with the difficulty of mental operations, for example during focused attention and information uptake, processing and learning or during memory recall. Theta frequencies become more prominent with increasing task difficulty. This is why theta is generally associated with brain processes underlying mental workload or working memory (Klimesch, 1996; O'Keefe & Burgess, 1999; Schack, Klimesch, & Sauseng, 2005). Theta is associated with a wide range of cognitive processing such as memory encoding and retrieval as well as cognitive workload [10]. Whenever we're confronted with difficult tasks (counting backwards from 100 in steps of 7, or when recalling the way home from work, for example), theta waves become more prominent. Theta is also associated with increased fatigue levels" [8] [11].

Alpha Band (8-13 Hz):

"Alpha is generated in posterior cortical sites, including occipital, parietal and posterior temporal brain regions. Alpha waves have several functional correlates reflecting sensory, motor and memory functions. One can see increased levels of alpha band power during mental and physical relaxation with eyes closed. By contrast, alpha power is reduced, or suppressed, during mental or bodily activity with eyes open. Alpha suppression constitutes a valid signature of states of mental activity and engagement, for example during focused attention towards any type of stimulus (Pfurtscheller & Aranibar, 1977). Whenever we close our eyes and bring ourselves into a calm state, alpha waves take over. Alpha levels are increased when in a state of relaxed wakefulness. Biofeedback training often uses alpha waves to monitor relaxation. They are also linked to inhibition and attention" [8] [12].

Beta Band (13-30 Hz):

"Oscillations within the 13 – 30 Hz range are commonly referred to as beta band activity (Niedermeyer & da Silva, 2012). This frequency is generated both in posterior and frontal regions. Active, busy or anxious thinking and active concentration are generally known to correlate with higher beta power. Over central cortex (along the motor strip), beta power becomes stronger as we plan or execute movements, particularly when reaching or grasping requires fine finger movements and focused attention. Interestingly, this increase in beta power is also noticeable as we observe others' bodily movements. Our brain seemingly mimics the limb movements of others, indicating that there is an intricate "mirror neuron system" in our brain which is coordinated by beta frequencies (Zhang et al., 2008). Over motor regions, beta frequencies become stronger as we plan or execute movements of any body part [13]. Interestingly, this increase in beta is also noticeable as we observe bodily movements of other people [14]. Our brain seemingly mimics their limb movements, indicating that there is an intricate "mirror neuron system" in our brain which is potentially coordinated by beta frequencies" [8].

Gamma Band (above 30 Hz):

"At the moment, gamma frequencies are the black holes of EEG research as it is still unclear where exactly in the brain gamma frequencies are generated and what these oscillations reflect. Some researchers argue that gamma, similar to theta, serves as a carrier frequency for binding various sensory impressions of an object together to a coherent form, therefore reflecting an attentional process. Others argue that gamma frequency is a by-product of other neural processes such as eye-movements and micro-saccades, and therefore do not reflect cognitive processing at

all. Future research will have to address the role of gamma in more detail. Some researchers argue that gamma reflects attentive focusing and serves as carrier frequency to facilitate data exchange between brain regions [15]. Others associate gamma with rapid eye movements, so-called micro-saccades, which are considered integral parts for sensory processing and information uptake"[8] [16].

1.5 How EEG works in the Human Brain:

"The brain is an electrical system – all of our thoughts (conscious or otherwise) are generated through a network of neurons, which send signals to each other with the help of electrical currents. The more electrical signals, the more neuronal communication, which corresponds to more brain activity.

The electrodes of an EEG headset can't detect changes in single neurons, but instead detect the electrical changes of thousands of neurons signaling at the same time.

The signal from the electrodes is then sent to an amplifier, that (no surprises here) amplifies the signal. A computer then receives this signal, and can generate various maps of brain activity, with a rapid temporal resolution.

A drawback for EEG is the spatial resolution – as the electrodes measure electrical activity at the surface of the brain, it is difficult to know whether the signal was produced near the surface (in the cortex) or from a deeper region"[17].

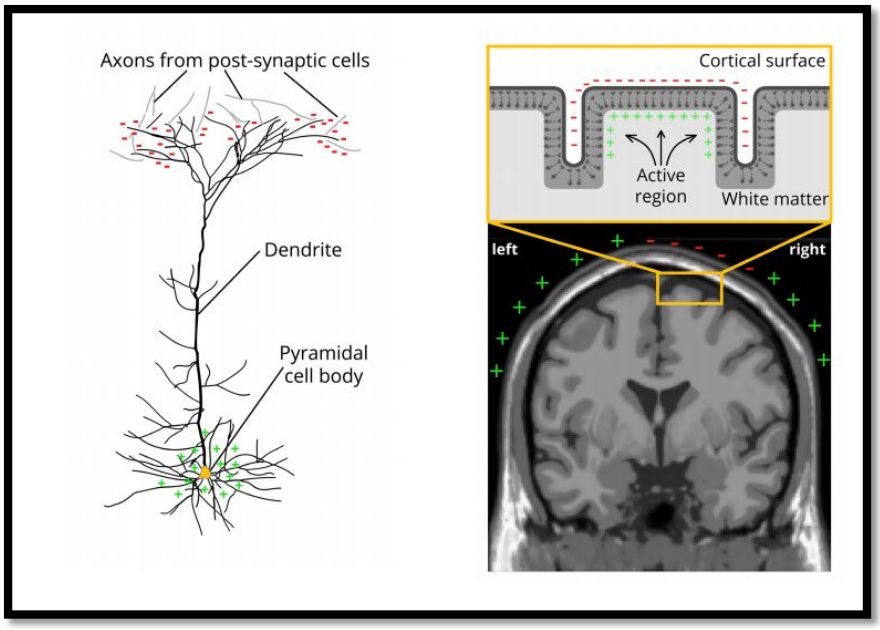

Figure 1.3: EEG signal generation at the scalp level from the triggering of the pyramidal cell by the release of neurotransmitter. (Reference: https://imotions.com/blog/eeg/)

"The brain consists of hundreds of thousands of cells, so-called neurons. In fact, there are about 100 billion neurons in the human brain, which are all heavily interconnected.

Neurons typically consist of a cell body and one or more dendrites which all end at synapses. Synapses act as gateways of inhibitory or excitatory activity between neurons. This means that synapses propagate information impulses across neurons (excitatory) or prevent the passage of information from one neuron to the next (inhibitory).

The synaptic transmission is triggered by the release of neurotransmitters (dopamine, epinephrine, acetylcholine, etc.), which causes a voltage change across the cell membrane. In other words: Any synaptic activity generates a subtle electrical field, which is also called postsynaptic potential (post = behind). Postsynaptic potentials typically last tens to hundreds of milliseconds"[17].

1.6 EEG compared to other brain imaging techniques:

"Magnetencephalography (MEG) records the magnetic fields generated by neural activity. Like EEG, MEG has excellent time resolution and is often considered to capture deeper neural activity much better than EEG. MEG scanners are large, stationary and expensive. They require heavy technical maintenance and training resources.

Functional Magnetic Resonance Imaging (fMRI) measures changes in blood flow associated with neural activity. Increased neural firing requires oxygen, which is delivered by blood, and the magnetic properties of oxygenated blood are different from those of non-oxygenated blood. This property is measured by fMRI as a distortion of the magnetic field generated by protons. fMRI has excellent spatial resolution while at the same time lacking the time resolution of EEG.

Functional Near-Infrared Spectroscopy (fNIRS) is a widely used non-invasive optical imaging technique which has the ability to measure cortical level activity based on hemodynamics in the brain. Moreover, cerebral blood flow differences in oxygenated hemoglobin (HbO_2) and/or deoxygenated hemoglobin (Hb) in different areas in the brain act as a biomarker of neuronal activation.

Positron emission tomography (PET) is an invasive nuclear imaging technique based on gamma radiation of a decay which is inserted into the body of the respondent. With PET, you can monitor metabolic activity (for example, glucose metabolism) of neurons during cognitive activity. While PET scans are much more robust towards motion artifacts, they are lacking the high time resolution of EEG recordings"[17].

CHAPTER 2
ECONOMIC DECISION MAKING USING EEG

2.1 Aim of the study:

The aim of this study is to understand scalp level EEG response changes associated with different task conditions of complicated decision making process. The root mean square (RMS) of EEG amplitude is measured as an index of the power content of EEG recorded from the motor cortical area. This provides an estimation of magnitude changes in the brain associated with different cortical functions, while the subject is doing complicated decision making tasks. Understanding scalp EEG and how it differentiates in different task conditions are the key goal of this study.

2.2 RMS (Root Mean Square) Power:

For feature extraction of EEG data, RMS plays a great role by providing a measure of the strength of the sample signal. The strength can be calculated by applying Root Mean Square (RMS) in the EEG data [18]. In mathematics, RMS is known as the quadratic mean. It is a statistical measure of the magnitude of varying quantity. RMS is useful when there are positive and negative variations, for instance sinusoid. RMS is one of the most commonly used methods that measure the amplitude of a bio - signal, e.g. audiological signals and electromyographic signals. The amplitude of a bio-signal expresses the magnitude of the power (energy per time) of that particular signal. Many studies have reported to calculate RMS magnitude of EEG signal for extracting the features during sleep study, muscle fatigue based on the following formula[18][19]:

The RMS for a collection f N values $\{x_1, x_2, \ldots, x_N\}$ is:

$$x_{rms} = \sqrt{\frac{1}{N}\sum_{i=1}^{N} x_i^2} = \sqrt{\frac{x_1^2 + x_2^2 + \ldots + x_N^2}{N}}$$

2.3 Methods:

Figure 2.1 shows an overall flow of the study, consisting of **four** major parts, which will be described in several sub-sections below. This analysis flow was followed for 64-channel data processing. The first section discuss the study design, and protocol, while the analysis of the 64-channel EEG is discussed in the followed by sections, of data recorded from 10-20 EEG electrodes.

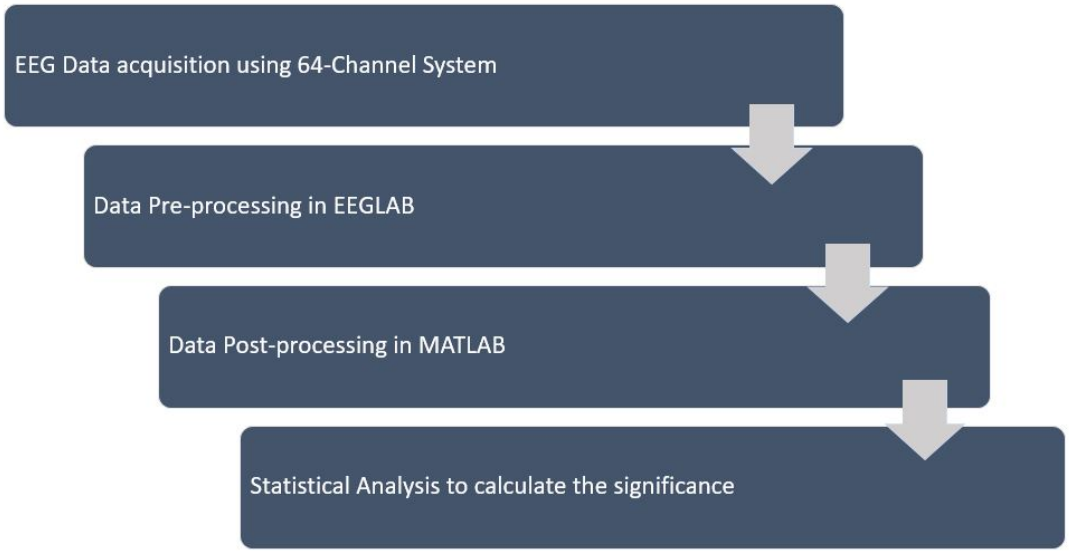

Figure 2.1: Overall flow of the study

2.3.1.Participants in the study:

A total of 13 healthy human participants (7 males, 6 females, age = 23 (±5) years) were recruited from the local community of the University of Texas at Arlington. The inclusion criteria included: either sex, any ethnic background, and in an age range of 18–28 years old. The exclusion criteria included: diagnosed with a psychiatric disorder, history of a neurological condition, history of severe brain injury, history of violent behavior, have ever been institutionalized/ imprisoned, current intake of any medicine or drug, or currently pregnant. The experimental protocol was approved by the institutional review board of the University of Texas at Arlington for the good clinical practice for the human subjects. Informed consent was obtained from each participant prior to the experiments.

2.3.2 Experimental Study Design & Procedures

2.3.2.1 Study Design:

The study is designed based on the Newsvendor Inventory Problem, where the news vendor must decide how many newspapers to buy each day at the wholesale price and to sell at the retail price. Moreover, this problem has some characteristics. The demand is uncertain but from a known distribution. The whole protocol consists 40 trials, where each person have a decision in every period of trials. There is a cost for ordering items ranging from 0 to 300. The number of items each time order is called *order quantity*. The subject must decide the order quantity for the inventory each trial. Each trial is independent of one another.

According to the newsvendor problem, let q be the order quantity, D be the unknown demand, c be the cost, p be the selling price and l be the left-over quantity. If $q > D$, the profit (P) is calculated as a function of q and D by the following equation [5]:

$$P(q, D) = (p - c)(\min(q, D)) - l * (p - c)$$

The protocol contains two independent treatments. The further details of the treatment are provided in Table 2.1. The subject was asked to enter the order quantity in between 0 and 300 depending on their previous trial experience even though it's coming from an unknown random demand, which was generated from a uniform distribution between 0 and 300. Each experiment consists of 40 trials. The price and cost were kept constant and known for each treatment. Subjects were randomly assigned for either high-margin or low-margin.

Treatment Type	**Low Margin**	**High Margin**
Price(P)	32	32
Cost(C)	24	8
Demand Range	[0 300]	[0 300]

Table 2.1: Summary of the different treatment conditions.

2.3.2.2 Experimental Protocol:

The study protocol was created on MATLAB software. The protocol was consisted of 4 main phases, namely- Baseline, Decision, Rest, and Feedback. After baseline, the whole process went for 40 trials. Baseline was 30 seconds. During this period, the subject didn't do any mental tasks other than just looking into the screen. Then, the protocol was moved to the decision phase, the subject was shown the screen for a maximum of 20 seconds with price, cost and demand range with a text box to enter the order quantity. During this phase, the subject chose a demand ranging

from 0 to 300 within 20 sec of time for each trial. When the subject entered the order quantity, the screen shifted to a "Rest" phase of 5 seconds. As soon as the 'Rest' phase was gone, the feedback phase appeared for 10 seconds. During the feedback phase, the summary was displayed with the results of the decision phase in terms of a history table including the profit they made in each trial and cumulative net profit. Then, the protocol proceeded to the next trial followed by 5 seconds of "Rest" phase. Figure 2.2 shows the schematic diagram of the study protocol. The treatment was randomly assigned to the subjects. All the profit/loss details were stored along with the corresponding time stamps in separate .mat files in MATLAB.

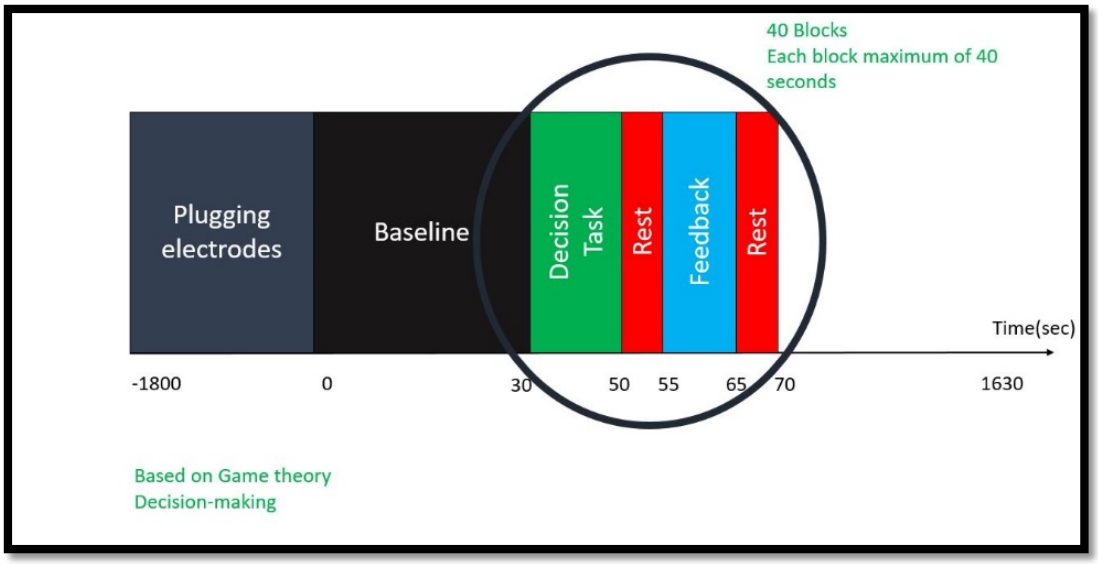

Figure 2.2: A schematic diagram of the experiment protocol.

2.3.2.3 MATLAB-based Game Theory Design:

The MATLAB version of the protocol has 4 phases. Figure 2.3 illustrates the exact 4 phases of the protocol in sequence: Baseline (30 sec), Decision (20 sec at most), Rest (5 sec), and Feedback (10 sec) respectively below:

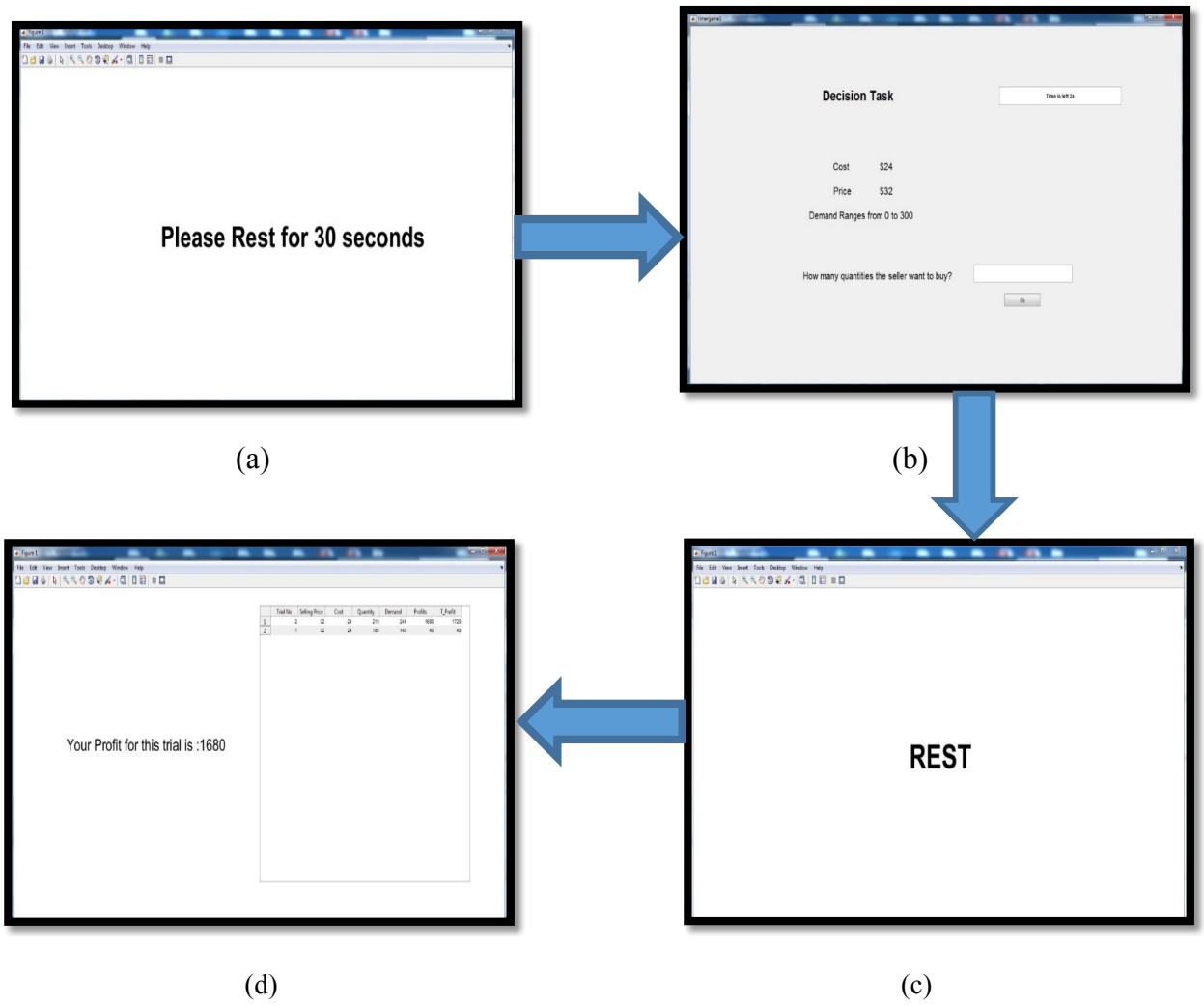

Figure 2.3: Screenshots of different phases for the MATLAB-based newsvendor game. (a) represents the baseline period to the participants for 30 seconds, and after this period decision-phase comes; (b) represents the decision-phase, where the subjects will enter their order quantity based on the cost and price of the product within 20 seconds, (c) represents the rest period of 5 seconds to the participants before they go to the (d) feedback phase, where the participants will see their profit/loss for the corresponding trial based on their chosen order quantity.

2.3.2.4 EEG Data Acquisition:

The whole setup was consisted of few key components employing an EEG recording system:

- Bio semi 64 channel electrode cap with 64 AgCl electrodes
- Amplifiers with filters

- A/D converter
- Recording device 1: EEG data are stored
- Recording device 2: Behavioral data are stored

As shown in Figure 2.4, the electrodes extracted the signals from the EEG-cap used in the head surface, while the subject was playing the Game-theory based Newsvendor Problem, the amplifiers amplified the microvolt signals into the range to be digitalized accurately, the converter changed the signals from analog to digital forms, and the personal computer stored and displayed the recorded data.

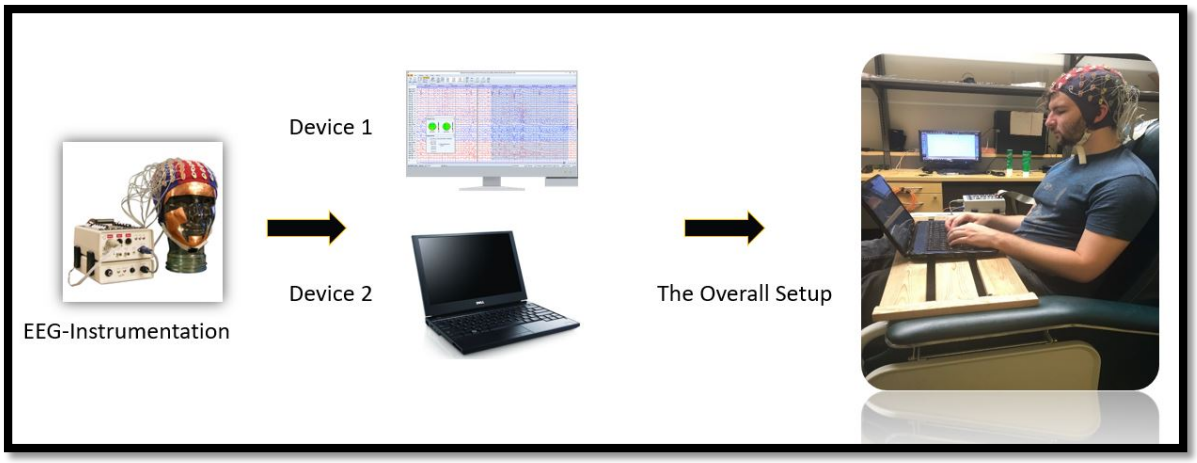

Figure 2.4: Experimental setup and data acquisition

In principle, as the voltage fluctuations measured at the electrodes are very small, the recorded data is digitized, and sent to an amplifier. The amplified data can then be displayed as a sequence of voltage values. The EEG recording electrodes and their proper functions are critical for acquiring appropriately high-quality data for interpretation. In my study, EEG signals were recorded with 64-channel Bio-Semi equipment according to the international 10–10 system with 64 AgCl electrodes mounted on top of the subject's head. Scalp electrodes consist of Ag-AgCl

disks, 1 to 3 mm in diameter, with long flexible leads that can be plugged into an amplifier. AgCl electrodes can accurately record very slow changes in potential. The multi-channel configurations can comprise up to 128 or 256 active electrodes.

Using the silver-silver chloride electrodes, the space between the electrode and skin should be filled with conductive paste or gel that also helps the electrode to stick. With a cap system, there is a small hole to inject the conductive paste, which serves as a medium to ensure small contact impedance at electrode-skin interface. The impedance of each electrode had to be less than 5 kΩ.

During the experiment, subjects were asked to sit in a comfortable chair (as shown in the figure 2.4), and all of their devices, keys or anything that can cause electromagnetic artifacts were kept away from the setup. Also, they were instructed to minimize body movements during EEG data acquisition. Computer based protocol was made in such a way to optimize the body movements using two button system. The EEG recordings were monitored by the research assistants on duty. Phones, radios or other electromagnetic devices were not allowed in the laboratory or on the subject for the duration of the experiment. They performed the game in randomly assigned treatment levels whereas 7 of them played high margin treatment, and 6 of them played the low margin one. One computer was used for recording the electrophysiological data and a laptop was used to play the game and to store the behavioral data throughout all subjects.

2.4 Data Analysis:

2.4.1 EEG Data Preprocessing:

After data acquisition, the 64-channel (N_e=64) EEG temporal profiles were exported to EEGLAB toolbox [20] for preprocessing. The data were recorded at 512 Hz(Sampling Frequency). First, a band-pass filter of 0.3 – 70 Hz (with windowed sinc high and low pass filters) was applied to the

EEG data for the removal of different unwanted signals, such as DC offset, system slow drifts, and any higher frequencies[26]. Specifically, a Blackman window between the high-pass transition band at 0.5 Hz and the low-pass transition band at 5 Hz were used for band-pass filtering Channels that were considered noisy, had extremely large amplitudes, and they were corrected using spherical interpolation. Then, notch filter was used for 60-Hz line noise removal using an EEGLAB plugin with default values [27]. Then, the data were subsequently average-referenced [22]. Next, ICA was applied to each subject's multi-channel EEG data to remove traditional artifacts of eye blinks, eye movements and muscle noise.[21] Finally, each subject's artifact-free data were separated in five frequency components, namely – Delta, Theta, Alpha, Beta, and Gamma for further processing. Figure 2.5 presents the pre-processing flowchart given below:

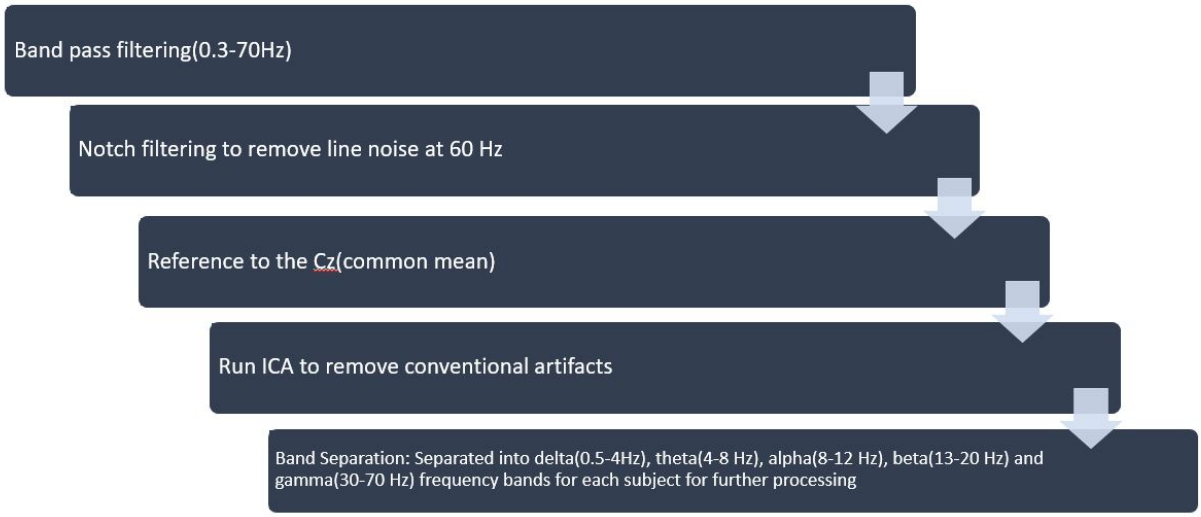

Figure 2.5: the entire data pre-processing steps/procedures from 64-channel EEG data acquisition to five frequency component separation.

2.4.2 EEG Data Post-Processing:

After preprocessing, each subject's individual band data were separated into three individual phases according to the recorded time-stamps from data acquisition. We call this step as 'Epoching'. For Baseline, last 15 seconds data were extracted for each subject, and it was then used for RMS power calculation for each EEG channel. Decision and feedback phases were consisted of 40 trials. Each subject's decision and feedback data were extracted according to the time-stamps and RMS power was calculated for each channel for each of those individual phases. The above mentioned procedures were done for each band separately. Baseline was corrected by subtracting the baseline data from decision and feedback. Then, each of the subjects' individual RMS data of baseline, decision, and feedback phases were averaged across 13 subjects for TOPOPLOT generation. Finally, topoplot function was used in MATLAB to generate the topoplots of the averaged baseline, decision and feedback for comparative study[25]. Figure 2.6 shows the post-processing steps illustrated below:

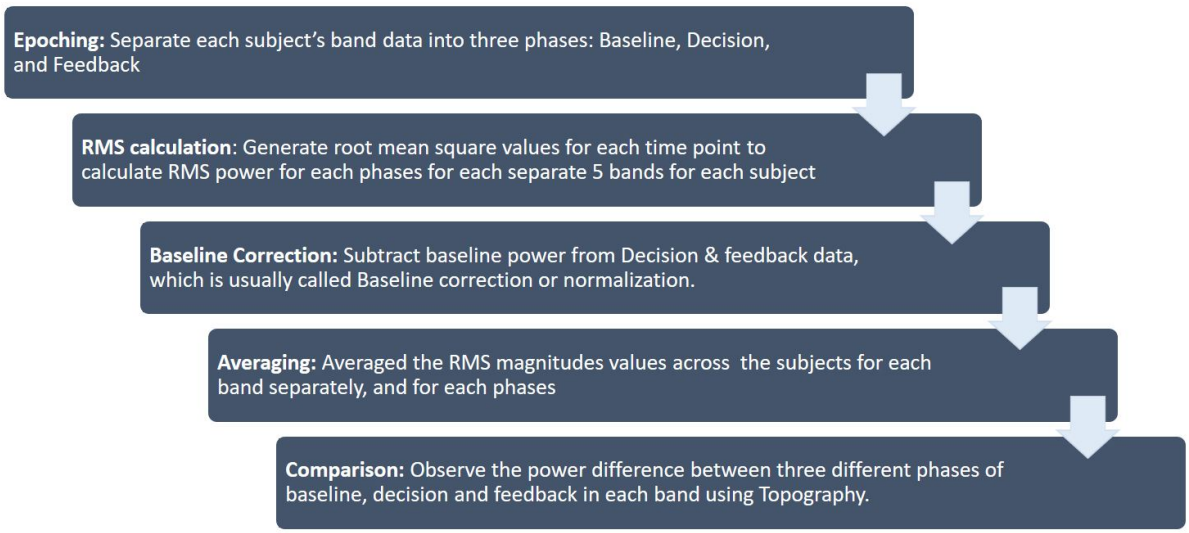

Figure 2.6: the flow-chart of EEG data post-processing in our study.

CHAPTER 3

RESULTS, OBSERVATION AND SPECULATION

3.1 Baseline Topoplots:

3.1.1 Observation:

From figure 3.1, it is explicit that average RMS power is varied throughout different components of EEG. Few observations can be concluded from the baseline topoplot. Usually in the baseline phase, subjects don't do any cognitive tasks other than looking into the screen for 30 seconds. Delta has more activation compared to all other bands. They do share close symmetrfical pattern throughout all frequency components. Alpha and Beta frequecny component shows some activation characteristics, primarily in the occipital side of the brain, which can be due to visual detection and memory processing.

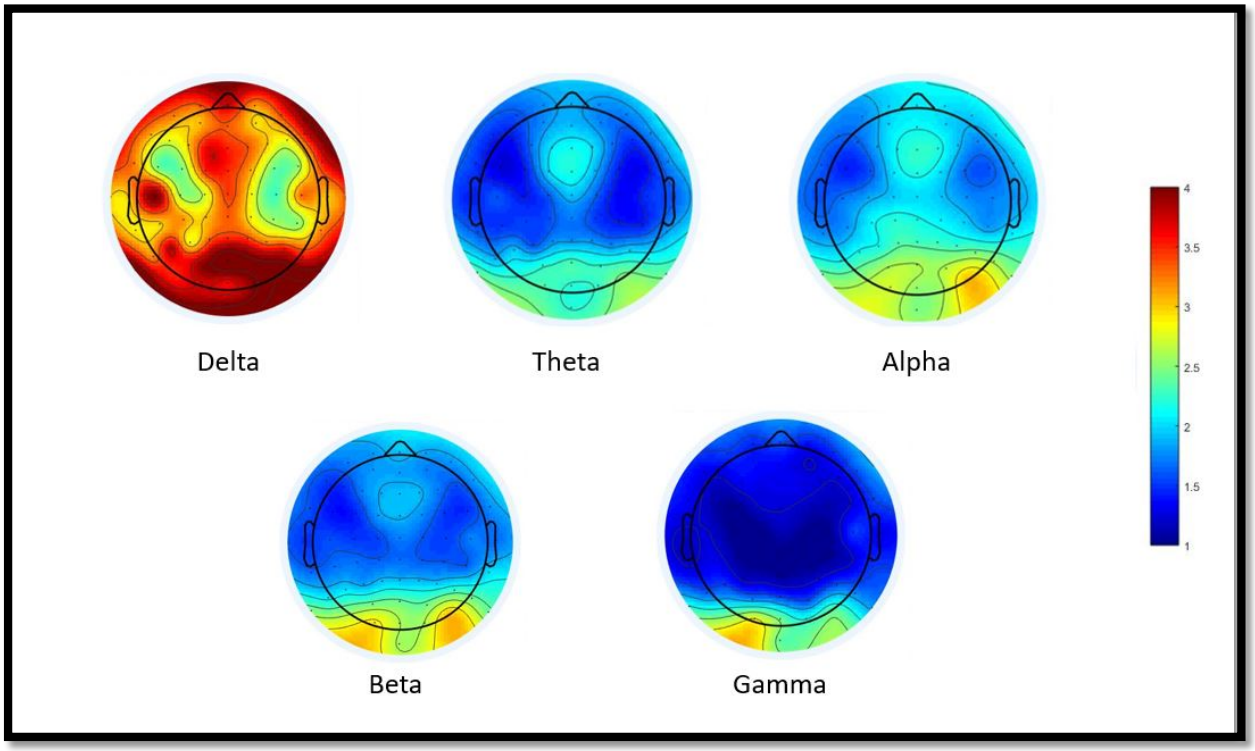

Figure 3.1: Average Topoplots of RMS magnitudes of Baseline(n=13) for five frequency components Delta(1-4 Hz), Theta(4-8 Hz), Alpha(8-13 Hz), Beta(13-30 Hz), and Gamma(30-70 Hz). The right colorbar represents the average rms magnitudes for each channel illustrated by an average topographical map. In the colorbar, red defines activation in the particular brain region, and blue defines deactivation in the corresponding brain region.

3.2 Decision Topoplots:

3.2.1 Observation:

From figure 3.2, it is explicit that average power is varied throughout different components of EEG during Decision Phase. All of the power topoplots are plotted based on baseline correction. Baseline correction means average power of all 64 channels of the Baseline are subtracted from the similar of Decision Phase, to investigate how much activation took place in Decision Phase compared to the baseline. Few observations can be concluded from the baseline-corrected Decision topoplot.

Theta seems more activated during decision making process, primarily in the occipital side of the brain. From theta wave characteristic, it is prevalent that it has some working memory function which can be the relevant reason for activation during decision-making. Previous studies reported that Theta correlates of memory retrieval and decision-making.

Delta shows significant activation in the broadmann areas, primarily in the agranular frontal side of the brain, which can be due to continuous attention-tasks, and working memory. Even few studies have reported that Delta oscillations reflect the linkage between parietal and frontal cortical circuits during decision-making, which is par with our findings [23]. It can be also observed that beta and alpha shows some decrease in the power value in decision-making process compared to the baseline.

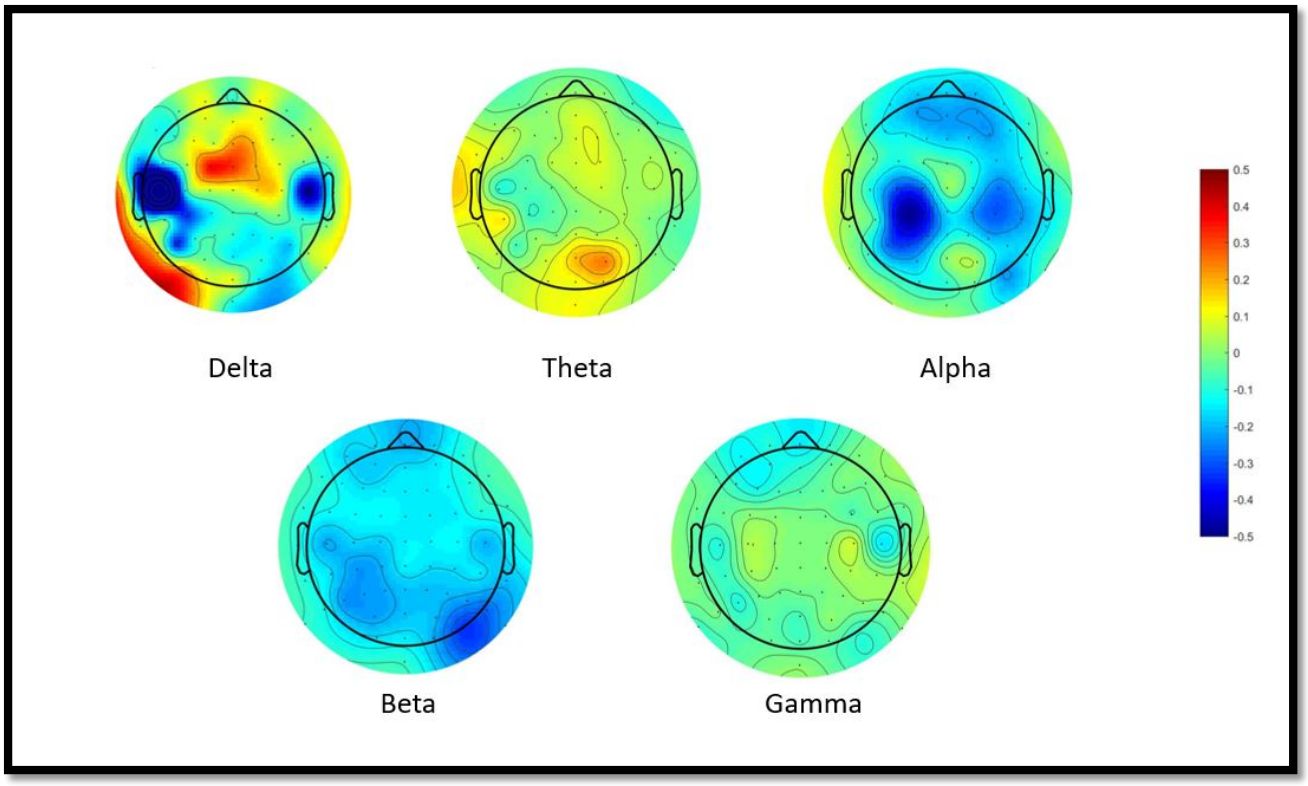

Figure 3.2: Average Topoplots of RMS magnitudes of Decision(n=13) for five frequency components Delta(1-4 Hz), Theta(4-8 Hz), Alpha(8-13 Hz), Beta(13-30 Hz), and Gamma(30-70 Hz). The right colorbar represents the average rms magnitudes for each channel illustrated by an average topographical map. In the colorbar, red defines activation in the particular brain region, and blue defines deactivation in the corresponding brain region.

3.3 Feedback Topoplots:

3.3.1 Observation:

From figure 3.3, it is explicit that average RMS power is varied throughout different components of EEG during Feedback Phase of the study. All of the power topoplots are plotted based on baseline correction. Few observations can be concluded from the baseline-corrected Feedback topoplot.

Delta seems less activated, which is quite relevant to the characteristic of the delta. Delta is primarily more activated in the continuous-attention based tasks. During feedback phase,

subjects are usually relaxed, not doing any tasks other than looking into the screen to check their corresponding profit/loss per trials. Alpha holds the similar characteristic, usually it reflects the relaxing nature of the brain. Interestingly, Alpha turns out to be more significant in our study. During feedback, alpha shows quite activation, which means the subjects are more relaxed in feedback phase. Considering other bands, Beta has a little activation. Little activation in Beta indicates stress, anxiety, and poor cognition, which can be due to low margin treatment in our study.

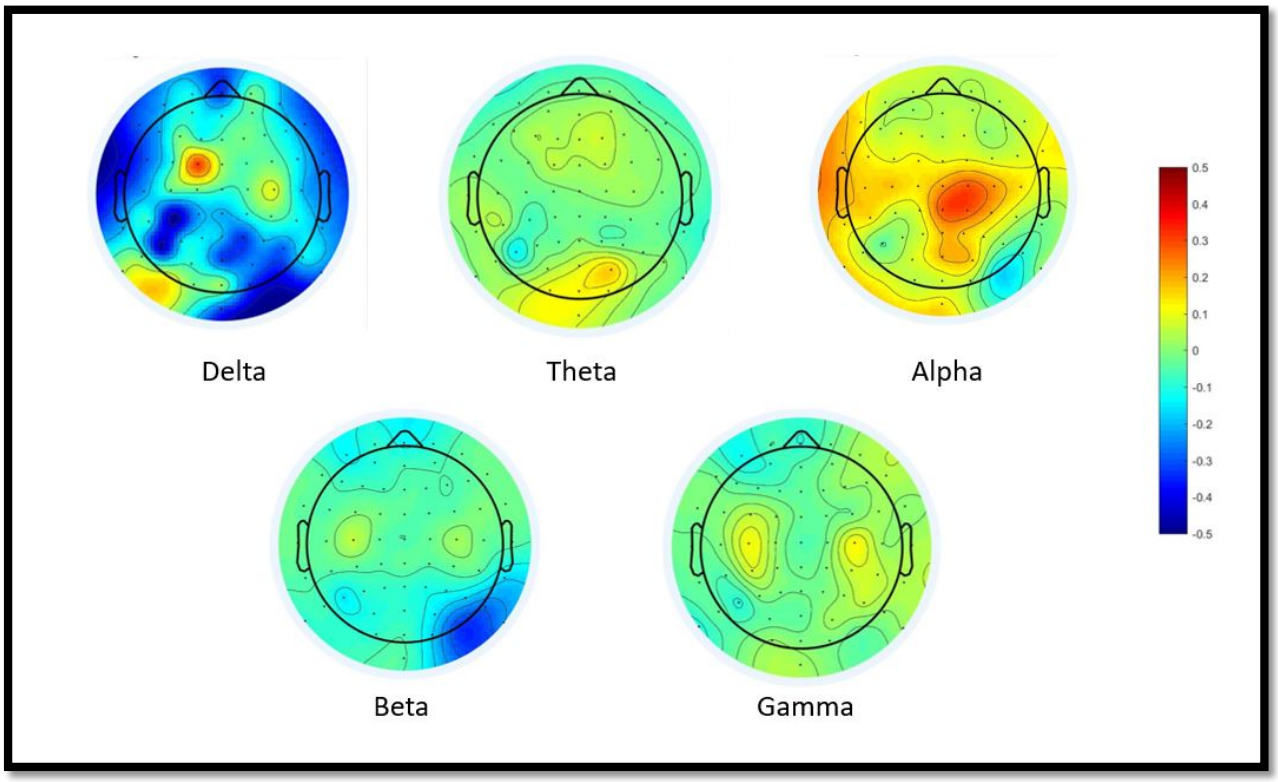

Figure 3.3: Average Topoplots of RMS magnitudes of Feedback(n=13) for five frequency components Delta(1-4 Hz), Theta(4-8 Hz), Alpha(8-13 Hz), Beta(13-30 Hz), and Gamma(30-70 Hz). The right colorbar represents the average rms magnitudes for each channel illustrated by an average topographical map. In the colorbar, red defines activation in the particular brain region, and blue defines deactivation in the corresponding brain region.

3.4 Statistical Analysis:

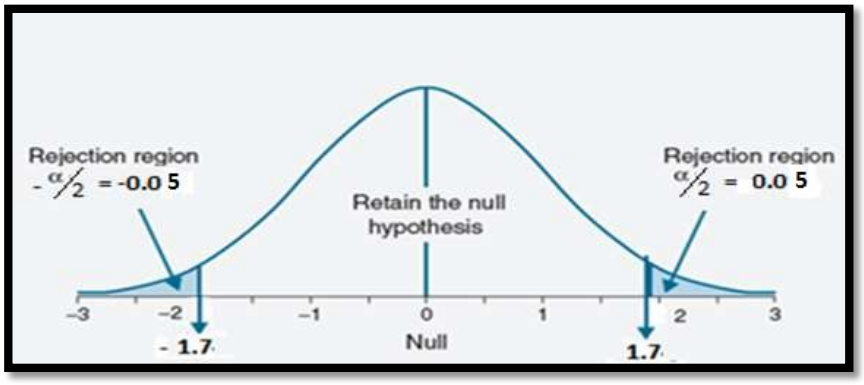

Figure 3.4: T-test bell curve

Each of the T-matrices is spread across the bell curve. Since we are only interested in finding the T-values that cause significant changes in brain connectivity at a certain state, a paired-sample T-test is performed between each of task conditions for all the subjects and the values are considered significant that were lying in the rejection region.

So, the test hypotheses can be formed as follows-

Null hypothesis: H0: $\mu 1 = \mu 2$; i.e. there is no significant differences in brain state in between two comparisons.

Alternate hypothesis: Ha: $\mu 1 \neq \mu 2$; there are significant differences in brain state in between two comparisons.

Paired-sample or student t-test has been conducted between each of the phase to identify the significant electrodes found in each case. The highest number of significant electrodes are found in Delta band between Decision and Feedback phase ($n = 45$, $p<0.05$). [34]

Regular Paired t-test	Alpha= 0.05		
	No. of Significant Electrodes		
	Decision	Feedback	Decision-Feedback
Delta	6	9	45
Theta	3	0	6
Alpha	1	1	40
Beta	58	17	39
Gamma	5	0	7

Table 3.1: represents the no. of significant electrodes generated from a paired-student-t-test between decision & baseline, feedback & baseline and for decision vs. feedback for each frequency bands.

3.4.1 FWER(Family-wise Error Rate):

To optimize the error ratio in the statistical analysis, FWER(Bonferroni-Corrected) paired t-test has been conducted[35]. However, Bonferroni-corrected result doesn't work best in our case, which can be due to the low number of sample size. Delta band shows 9 significant electrodes between Decision and Feedback phase only, whereas only 2 significant electrodes are found in Beta band between Decision and Baseline.

Bonferroni Corrected	Alpha= 0.05/64=0.00078		
	No. of Significant Electrodes		
	Decision	Feedback	Decision-Feedback
Delta	0	0	9
Theta	0	0	0
Alpha	0	0	0
Beta	2	0	0
Gamma	0	0	0

Table 3.2: represents the no. of significant electrodes generated from a Bonferrnoi-corrected paired- t-test between decision & baseline, feedback & baseline, and for decision vs. feedback, for each frequency bands.

3.4.2 FDR (False Discovery Rate):

To acquire more precise and correct results, by eliminating all possible false positives, FDR provides a useful measure in statistics. More documentation related to FWER and FDR are provided in Chapter-5(appendix section).

Benjamini-Hochberg False Discovery Rate Procedures:

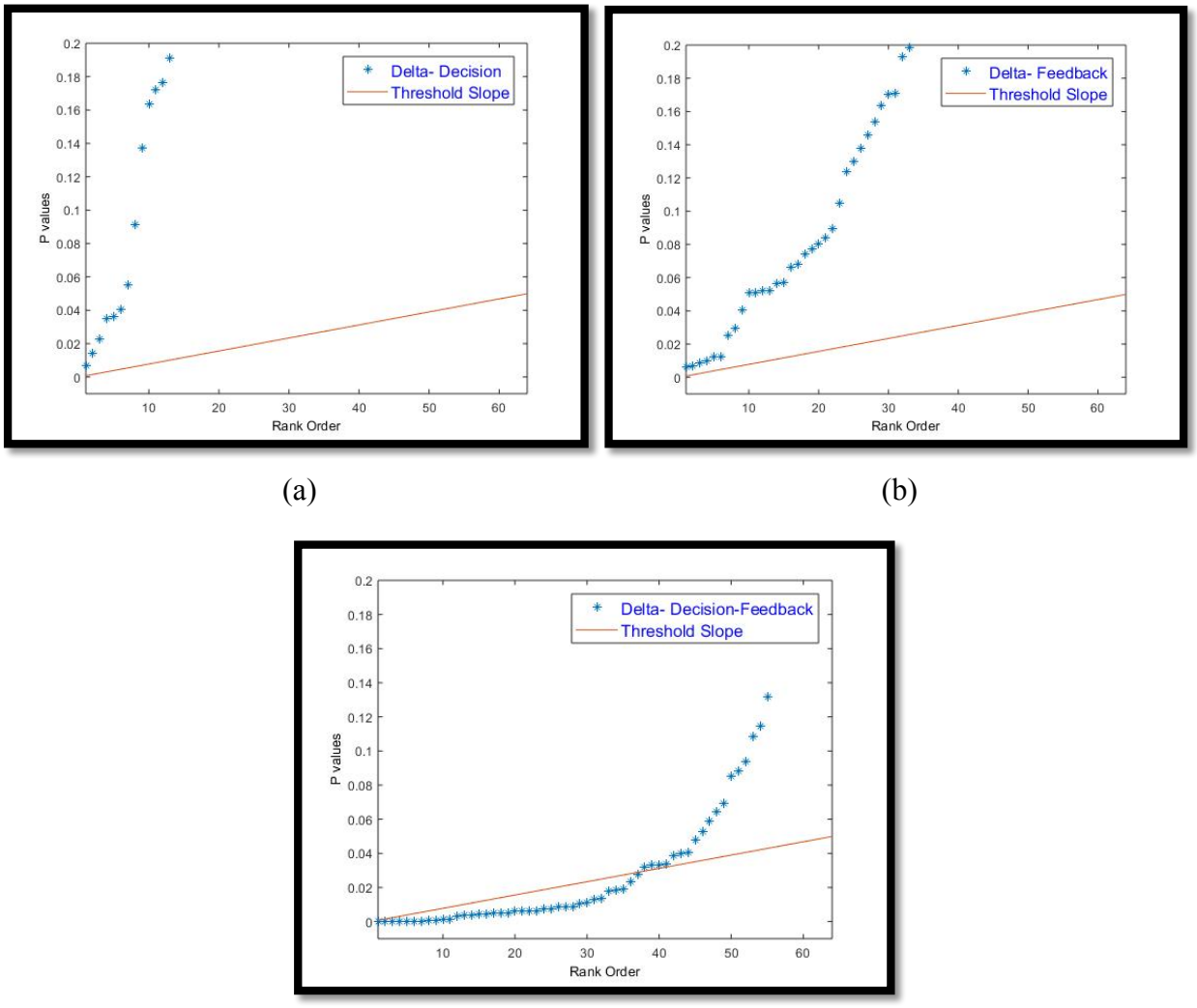

(a) (b)

(c)

Figure 3.5 illustrates an example of FDR correction procedure for Delta band. x-axis represents the ranking order of the p-values generated from paired-t-test between each phase condition, and y-axis represents the p-values. The slope of the threshold (e.g 0.05 for our case) is indicated by the straight line (orange color). Any p-values below the threshold curve are the FDR-significant p-values, corresponding

to the significant electrodes. All the figures for FDR correction of other bands are included in the appendix section. (a) showing no significant p-values (corresponding electrodes) between Decision and Baseline, (b) showing no significant p-values (corresponding electrodes) between Feedback and Baseline, and (c) showing 37 significant active electrodes only during decision and feedback task.

Based on the electrodes found significant under FDR condition for each of the task-phase, the following table is formed.

FDR	Alpha= 0.05			
	No. of Significant Electrodes			
	FDR Threshold		FDR Threshold	Corrected
	Decision	Feedback	Decision-Feedback	
Delta	0	0	37	37
Theta	0	0	0	0
Alpha	0	0	0	40
Beta	58	0	0	30
Gamma	0	0	0	0

Table 3.3: represents the no. of significant electrodes generated from a paired-student-t-test (FDR-corrected) between decision & baseline, feedback & baseline and for decision vs. feedback for each frequency bands.

Interestingly, only Delta shows a significant number of electrodes between Decision and Feedback phase ($p<0.05$, FDR-corrected). And, Beta band shows significance almost everywhere ($n=58$ electrodes) in Decision phase (compared to the baseline). So, beta band might have some statistically significance in decision-making. It is observed that not any significant electrodes are found for any of the bands other than Delta between Decision and Feedback phase for FDR-threshold($p<0.05$). However, the highest number of electrodes ($n=40$ electrodes) are found in Alpha Band, for corrected FDR-threshold ($p<0.08$). 30 electrodes are found statistically significant under FDR-corrected threshold ($p<0.08$) for Beta band between Decision and Feedback phase.

3.5 Clustering:

FDR provides quite a few significant electrodes for Delta, Alpha and Beta bands, which are true positive. [36] Among all the significant electrodes found by FDR-correction in Delta, Alpha, and Beta Bands, the most common electrodes are used for clustering. The neighboring electrodes are taken into account, for sectioning them into 5 clusters manually.

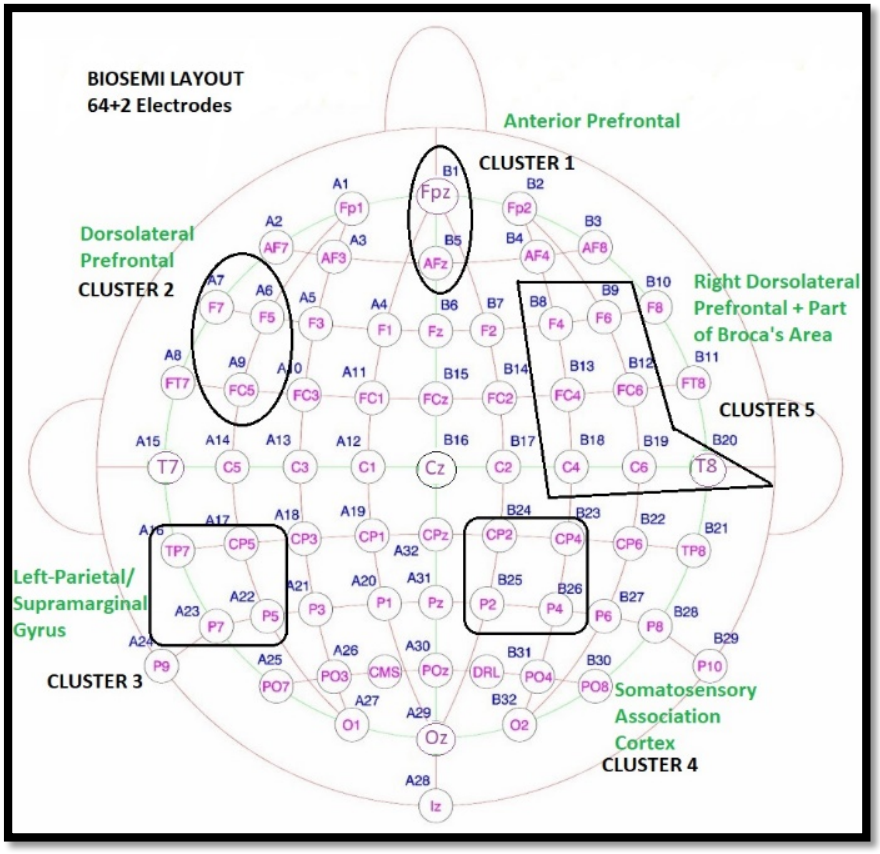

Figure 3.6: A Biosemi layout of 64 electrodes representing five clusters. This figure illustrates the layout of the five clusters, which are made based on the neighboring electrodes found in paired-t-test(FDR-corrected), in Biosemi layout(64+2).

3.5.1 Paired-Student t-test:

To verify the significance of the clusters under FDR, paired-student t-test has been conducted between Decision and Feedback phase. We are more interested into the power comparison of these two task conditions among these 5 clusters for 3 significant bands. Since, all the clusters are made based on the significant electrodes found in three bands, we will be only focusing on these three bands here. The total power of each cluster for decision and feedback phase are considered as two input vectors for conducting paired-t-test. All the p-values are plotted in the table for each cluster and for each frequency band.

p-values					
	Cluster 1	Cluster 2	Cluster 3	Cluster 4	Cluster 5
Delta	0.0134	0.0186	0.00062	0.0238	0.0264
Alpha	0.0648	0.0204	0.038	0.0101	0.1226
Beta	0.02318	0.0108	0.038	0.0272	0.0178

Table 3.4: P-values generation for each cluster and for each frequency bin. This table illustrates the p-values generated from a paired-student-t-test between decision and feedback phase for five clusters, and for each frequency band.

3.5.2 FDR Plots: To verify the significance of the clusters, all the p-values are plotted under FDR condition to check which clusters are significantly showing difference among Decision and Feedback task.

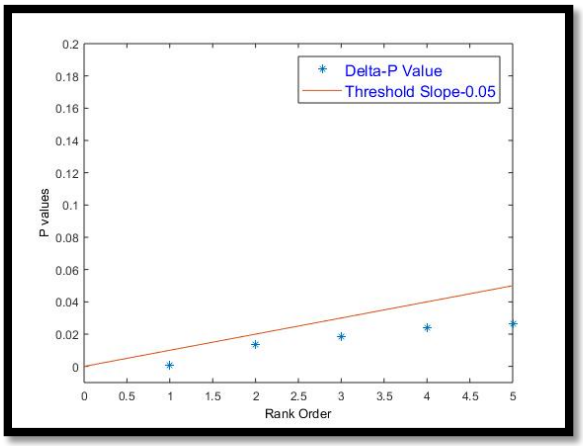

(a)

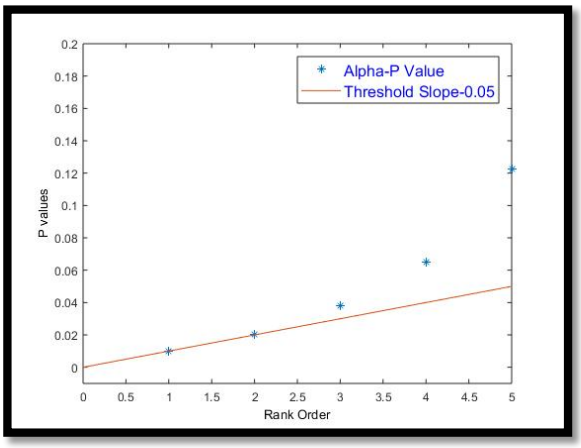

(b)

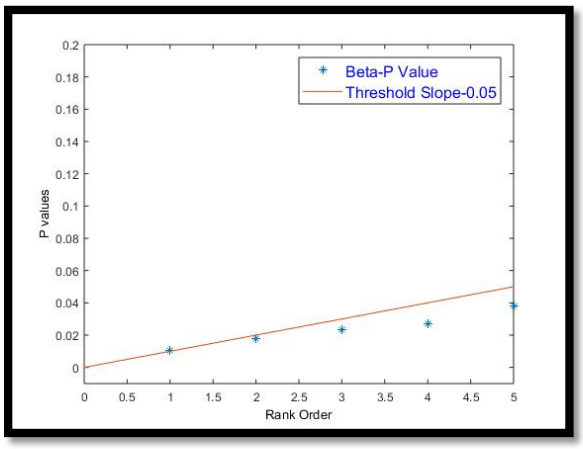

(c)

Figure 3.7: illustrates five FDR-corrected plots for each band. x-axis represents the ranking order(smallest to largest) of the p-values generated from paired-t-test between decision and feedback for 5 clusters, and y-axis represents the p-values for each cluster. The slope of the FDR-threshold (e.g 0.05- for our case) is indicated by the straight-line(orange color). Any p-values below the threshold curve are the FDR-significant p-values, corresponding to the significant clusters. (a)

Based on the significant clusters found under FDR, the following table is formed and the p-values are marked to identify the significant clusters.

	p-values				
	Cluster 1	Cluster 2	Cluster 3	Cluster 4	Cluster 5
Delta	0.0134	0.0186	0.00062	0.0238	0.0264
Alpha	0.0648	0.0204	0.038	0.0101	0.1226
Beta	0.02318	0.0108	0.038	0.0272	0.0178

Table 3.5: Significant clusters-marked from FDR-correction. The green box (rectangular and circle) represents the significant p-values of corresponding clusters for each bands. The red rectangular box represents the p-values for Cluster 2 and Cluster 4, which are showing significance for all three bands.

In table 3.5, it is observed that Cluster 2 and Cluster 4 is almost significant for all 3bands. Cluster 1, 3, 4 are showing significantly difference between decision and feedback for 2 bands. Delta and Beta have observed significance for all five clusters, whereas Alpha band is showing significance for two clusters, specifically cluster 2 and cluster 4.

3.5.3 Clustering: Power Comparison:

3.5.3.1 Delta Band:

3.5.3.1.1 Observation:

From the bar-plot in figure 3.8, it is easily observable that all clusters are showing significant difference, even though most of them have significant decrease in power compared to baseline for decision and feedback phases. All the error bars are based on the standard error of the mean

in all comparisons. Cluster 1 is showing some positive activation in decision phase, whereas Cluster 5 is showing significant deactivation in feedback phase compared to baseline.

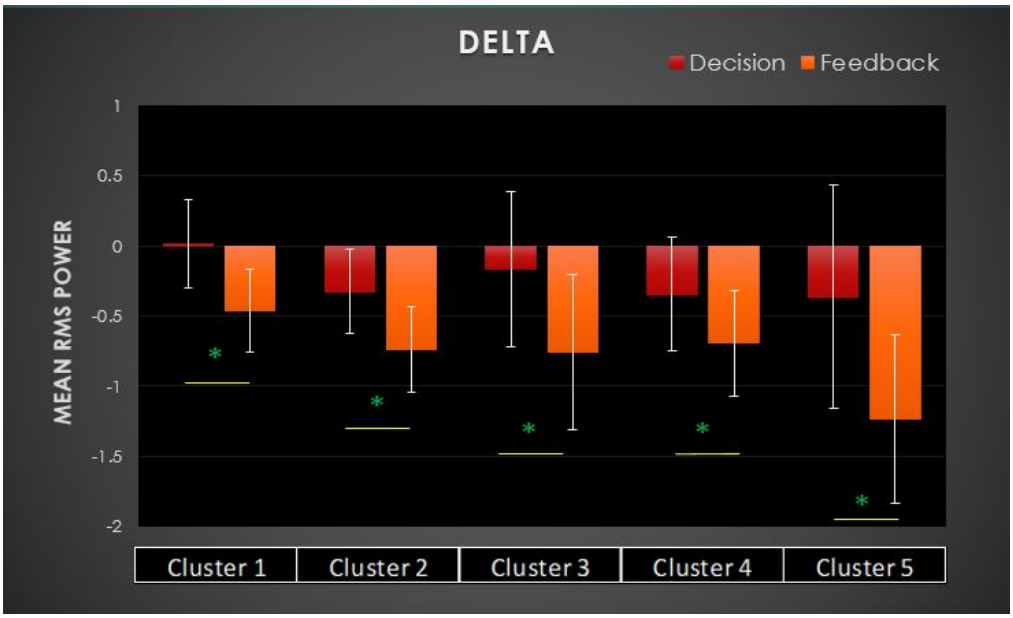

Figure 3.8: Mean RMS power comparison of Decision-making and Feedback Phase for five clusters for Delta band. The error bar is based on the standard error of the mean, and the '' represents the significance under FDR correction between decision-making and feedback phase for all clusters.*

3.5.3.2 Alpha Band:

3.5.3.2.1 Observation:

From the figure 3.9, it is observed that Alpha band is showing significant activation for all five clusters for feedback phase. On the other hand, decision-making is showing significant deactivation for all five clusters. Alpha is showing quite the opposite nature compared to Theta. From the characteristic of Alpha wave, we know that Alpha reflects the relaxation nature or resting state of the brain. Our findings suggest that Alpha become more prominent in activation

during the Feedback phase, which is quite relevant to the nature of feedback phase. Feedback phase is considered as the recovery/relaxation phase, where the subjects didn't do anything other than checking their profit/loss corresponds to each trial.

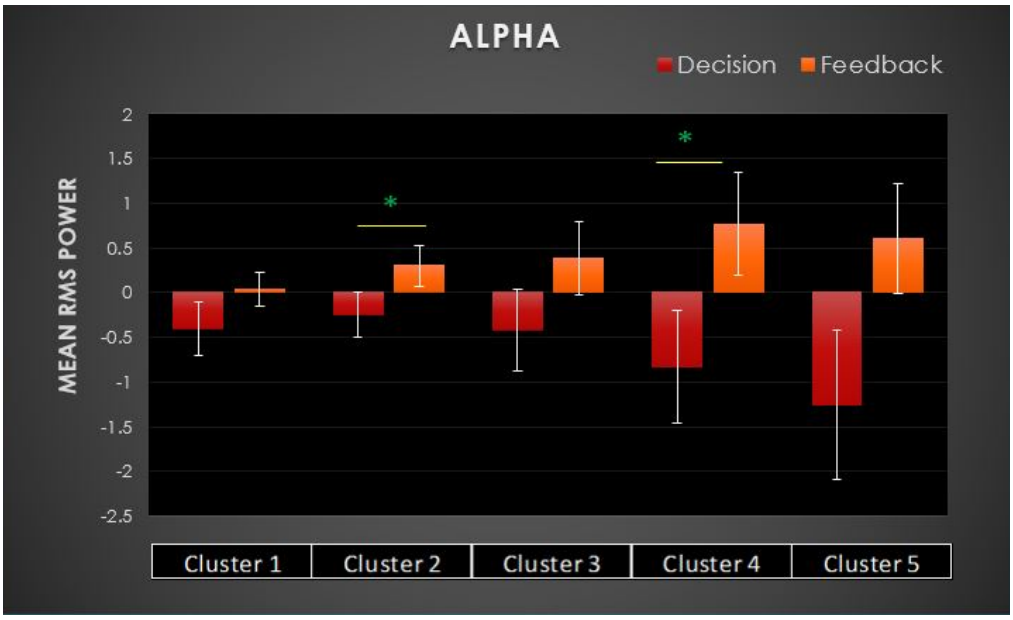

Figure 3.9: Mean RMS power comparison of Decision-making and Feedback Phase for five clusters for Alpha band. The error bar is based on the standard error of the mean, and the '' represents the significance under FDR correction between decision-making and feedback phase for two clusters.*

3.5.3.3 Beta Band:

3.5.3.3.1 Observation:

From the figure 3.10, the power comparison plot of Beta band, it can be stated that Beta band has significant deactivation in both of the decision-making phase and feedback phase. Even though,

all five clusters are turned out to be statistically significant ($p<0.05$, FDR-corrected), power difference can't be observed explicitly for Beta rhythm. The RMS magnitudes of Decision and Feedback phase are showing significant decrease compared to the Baseline. However, splitting Beta data into low-margin and high-margin treatment conditions, it is showing some interesting result.

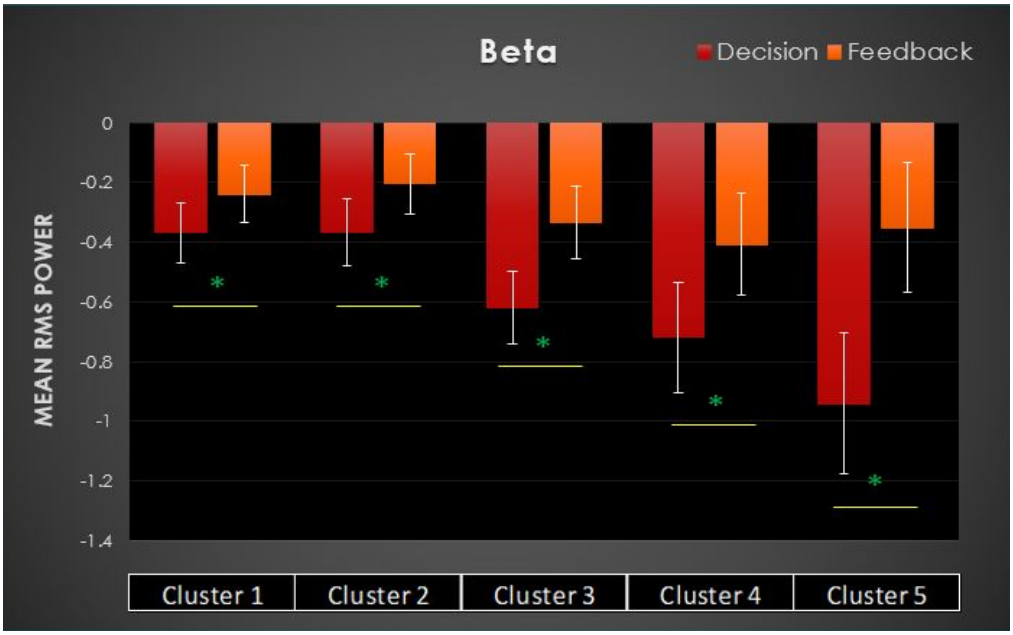

Figure 3.10: Mean RMS power comparison of Decision-making and Feedback Phase for five clusters for Beta band. The error bar is based on the standard error of the mean, and the '' represents the significance under FDR correction between decision-making and feedback phase for all clusters.*

The average topographical maps of Beta-low margin and Beta-high margin conditions are illustrated below for comparative study.

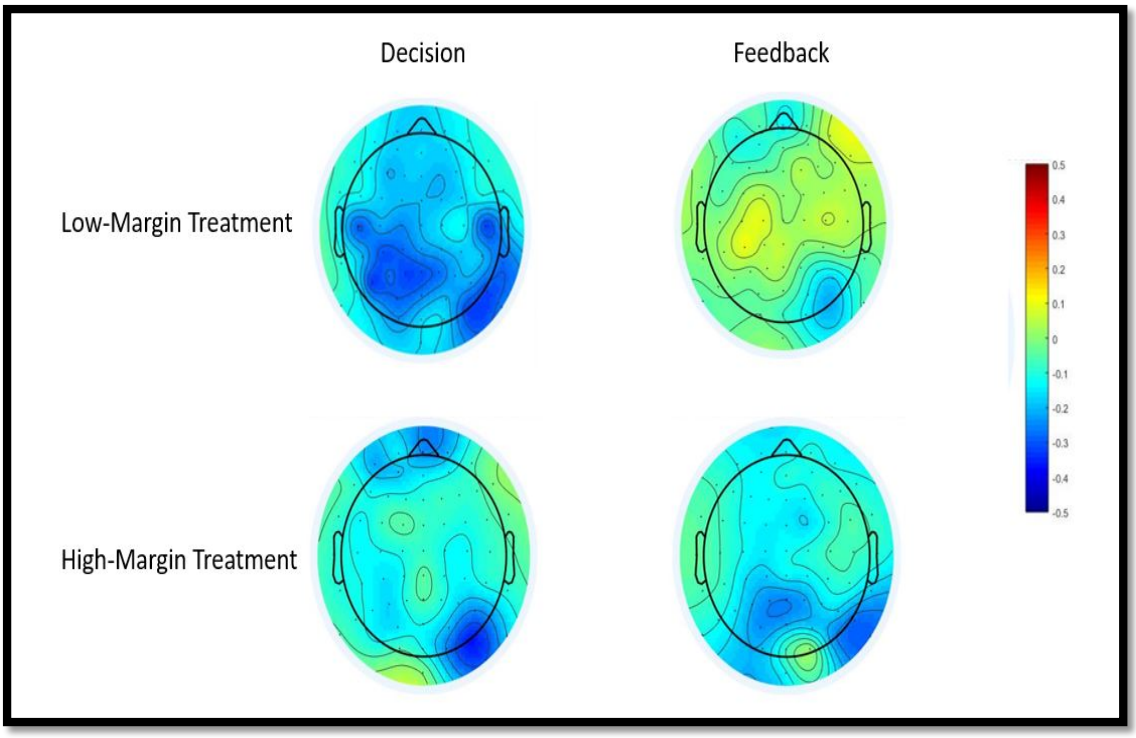

Figure 3.11: Average topographical maps of Beta band for decision and feedback phase under low-margin and high-margin treatment condition.

3.5.3.3.2 Power comparison:

3.5.3.3.3 Observation:

From the topographical maps in figure 3.11 and power comparison plots of Beta in figure 3.12, it is significantly observed that Beta band has significant deactivation for decision and feedback phase compared to the baseline for both treatment conditions. We have observed that Beta doesn't show much significance in power comparison in general. However, it shows some activation in feedback phase in cluster 5, and very little activation in cluster 3 for low-margin treatment condition. From the topographical point of view, some activation is observed in

feedback phase in cluster 5 for the low-margin treatment, which is primarily located around right dorsolateral prefrontal cortex.

Figure 3.12: Mean RMS power comparison of Decision-making and Feedback Phase for five clusters for Beta band under low-margin and high-margin treatment.

3.5.3.3.4 Discussion:

From the characteristic of Beta band, activation in right dorsolateral prefrontal cortex can be due to mental stress or anxiety in the feedback phase under low-margin treatment. Moreover, previous studies reported that increased power of feedback-induced beta oscillation reflects the omission of rewards relative to the reception of rewards [24]. During low-margin treatment condition, subjects were encountered with reward processing in feedback phase, and gaining reward in low-margin treatment is much difficult comparing to the high margin treatment. Our findings indicate that Beta has some activation in feedback phase for low-margin condition, which can be due to omission of rewards or can be due to mental stress of arithmetic processing.

CHAPTER-4

DISCUSSION & FUTURE WORK

4.1 Summary:

My goal of this study was to investigate the changes in electrophysiological signals in response to the newsvendor decision-making and feedback. This study has shown that EEG topoplot analysis can be adapted to investigate power across different regions of the brain during decision-making and feedback task conditions [25].

The 64-channel EEG data was preprocessed using EEGLAB platform in MATLAB, where all the datasets went through various types of filtering, ICA analysis to have artifacts-free electrophysiological data. Each datasets were separated into five individual frequency bands, and epoched into three separated events for further processing. Among these events, we were primarily interested into decision-making phase and feedback phase to investigate changes of the magnitudes or power of the signals across different subjects for these task conditions. Identification of significant electrodes observed in this study was an important step to locate the activation of brain-regions for different task conditions. Cluster-based analysis helped us to observe more significant activation occurred in the dorsolateral prefrontal cortex at four different brain rhythms. Topoplot analysis helped us to indicate the strengths of different brain-regions during this complicated decision-making process.

Several interesting observations have been observed for each of these task conditions through RMS topoplot and statistical analysis.

RMS Magnitude/Topographical point of view:

In short, Theta band shows significant activation in decision-making. Theta correlated in memory retrieval and decision-making. Alpha is more activated in Feedback, which corresponds to the most relaxing behavior. And, during decision-making, it shows the quite opposite nature. Beta doesn't show much activation. However, breaking Beta into low-margin and high-margin treatment, it shows some difference. Right Dorsolateral Prefrontal is activated in the feedback phase for Beta, which might be due to stress or anxiety in the feedback phase of low-margin treatment.

Statistical Point of View:

The highest no. of significant electrodes are found in Delta band from paired t-test. However, FDR results shows that Alpha has the most number of significant electrodes, (n=40). Delta has 37, and Beta shows 30 significant electrodes after FDR correction. Among the Clusters, Cluster 2 and Cluster 4 are showing most significant difference (significant for all 3 bands) between Decision and Feedback. Cluster 2 is located in Broadmann Areas 46, called as Dorsolateral Prefrontal Cortex (DL-PFC). Previous Studies reported that **Dorsolateral-Prefrontal** is mainly responsible for decision-making [6]. Some other associated functions relevant to our decision-making study[30]:

- Working memory
- Internal mental calculation
- Processing emotions and self-reflections in decision making.

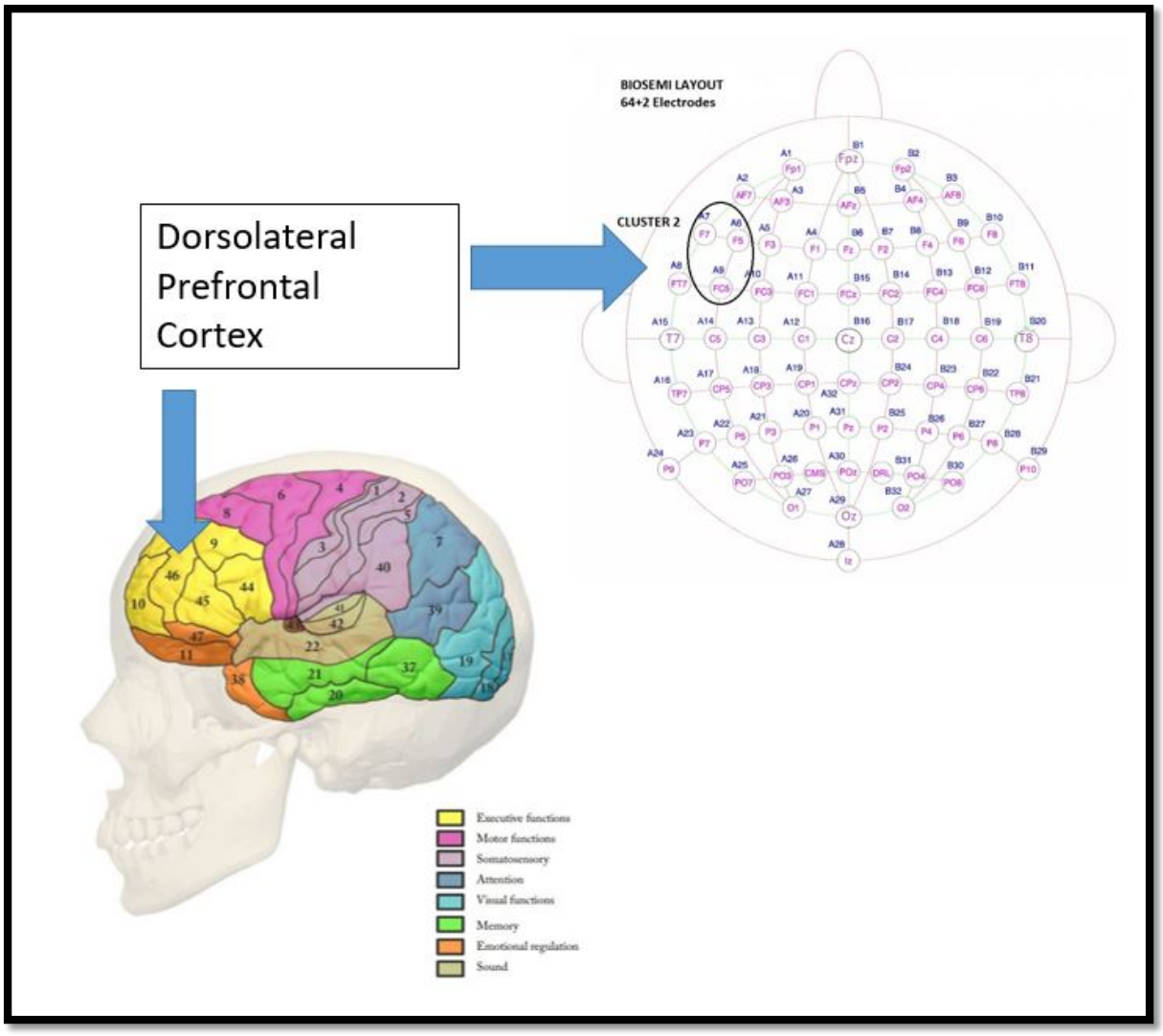

Figure 4.1: Area under Cluster 2 and its corresponding brain region in Broadmann areas. Dorsolateral Prefrontal Cortex is primarily located at Broadmann area 46, and it is prominent for its executive functions.

Cluster 4 is located at Somatosensory Association Cortex. This particular area includes superior parietal lobe (area 5 and area 7), and inferior parietal lobe (area 39 and area 40). Some associated function of this cluster: Processing emotions and self-reflections during decision-making (area 7), conscious recollection of previously experienced event, and working memory [30].

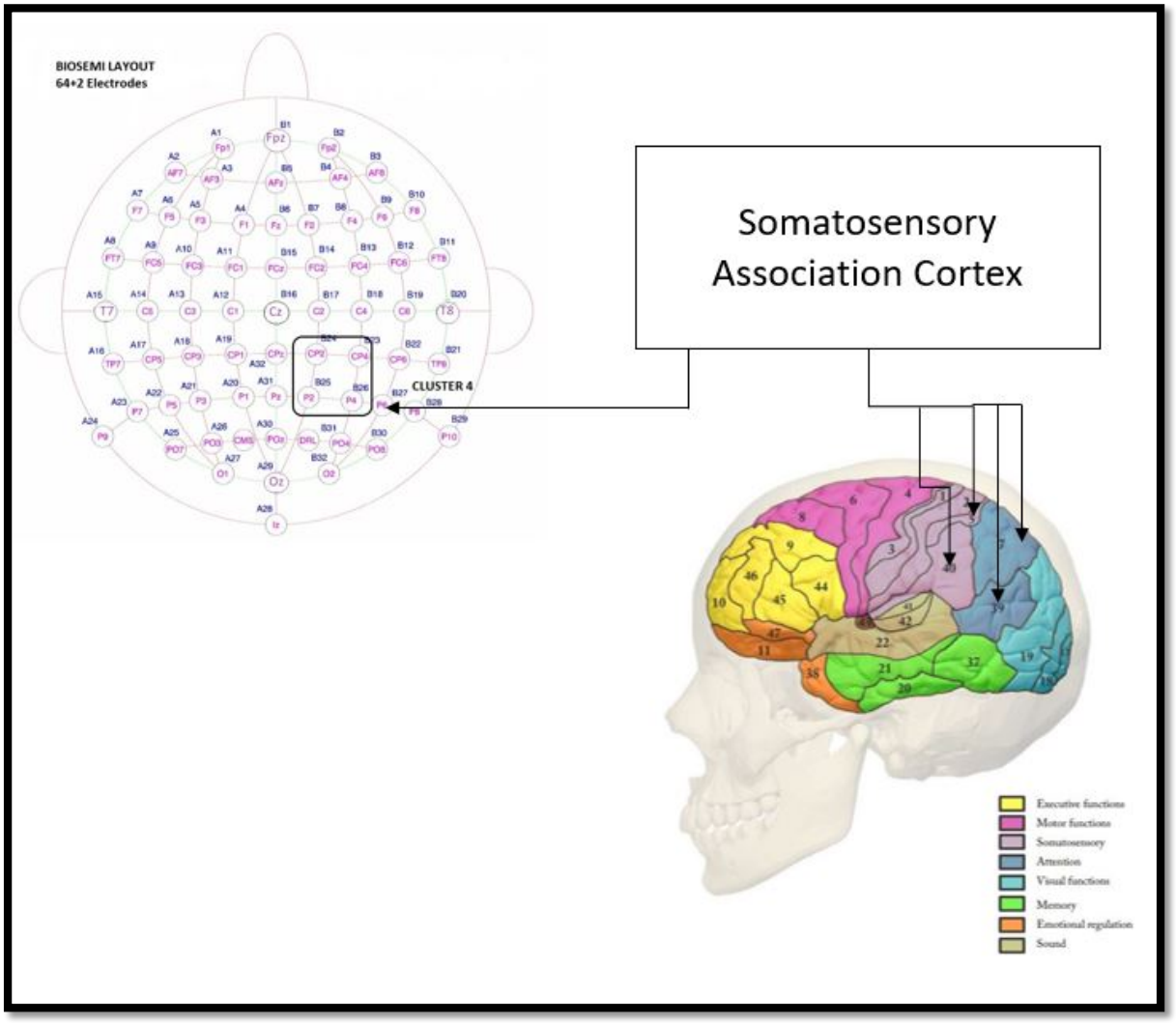

Figure 4.2: Area under Cluster 4 and its corresponding brain region in Broadmann areas. Somatosensory Association Cortex is primarily located at Broadmann areas 5,7,39 and 40. These particular areas are prominent for attention and visuals related functions.

Cluster 1, 3, and 5 have the second most significance, exactly in 2 bands. Cluster 1 is Broadmann areas 9L and 10L, which is roughly equivalent to Dorsolateral/Anterior Prefrontal Cortex. This area has a significant participation in memory- primarily memory encoding, memory retrieval, and working memory. It also shows other associate functions like-mental calculation, processing emotions, and self-reflections in decision-making (left) [30].

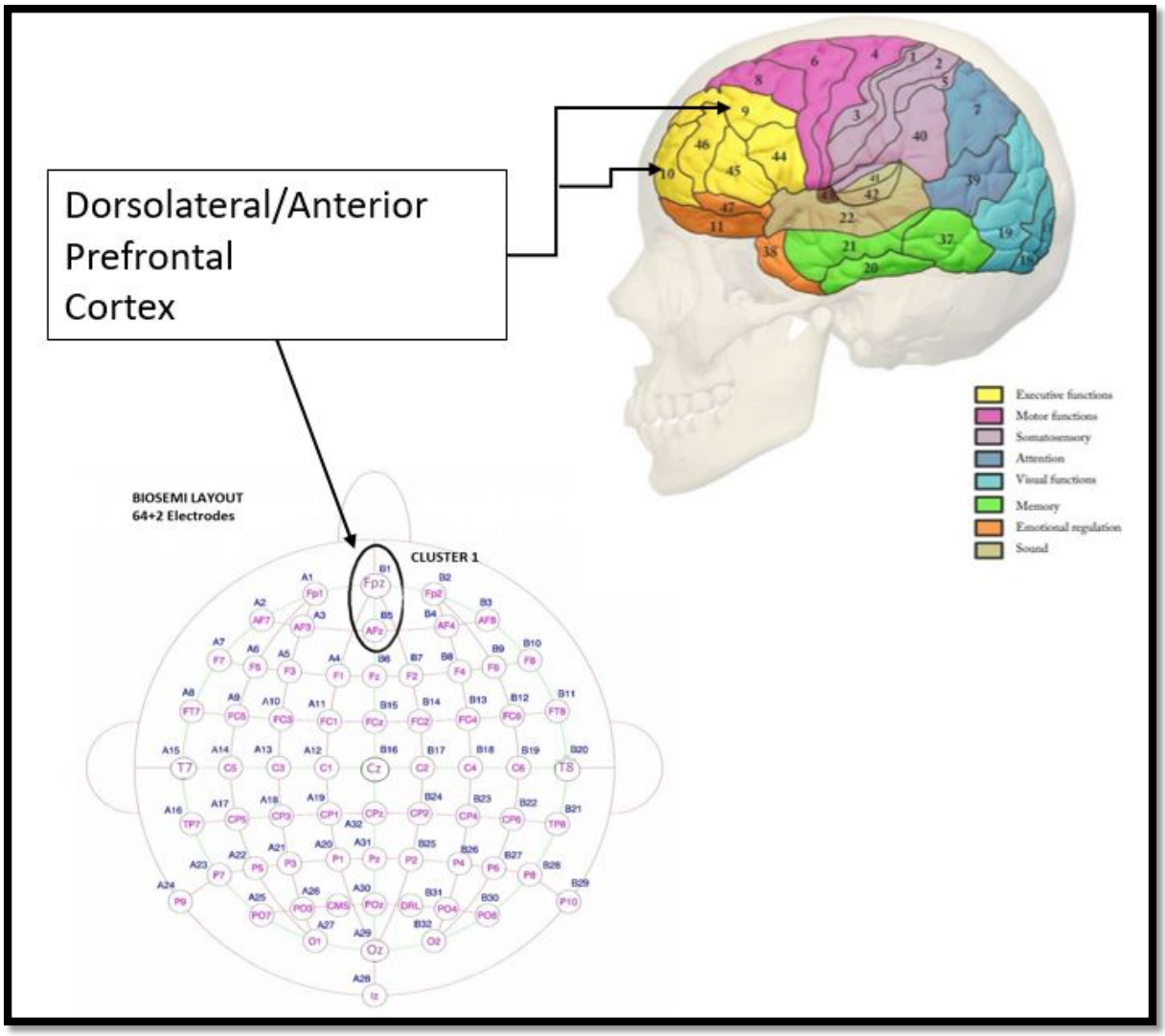

Figure 4.3: Area under Cluster 1 and its corresponding brain region in Broadmann areas. Dorsolateral/Anterior Prefrontal is located at Broadmann area 9 and 10, and this area has some executive functions in the brain.

Cluster 3 is primarily located in Broadmann areas 37, 39, and 40. All of these areas have common functionality in the brain, such as- single letter processing, calculation (integer computation), arithmetic learning, and performing creative tasks [30].

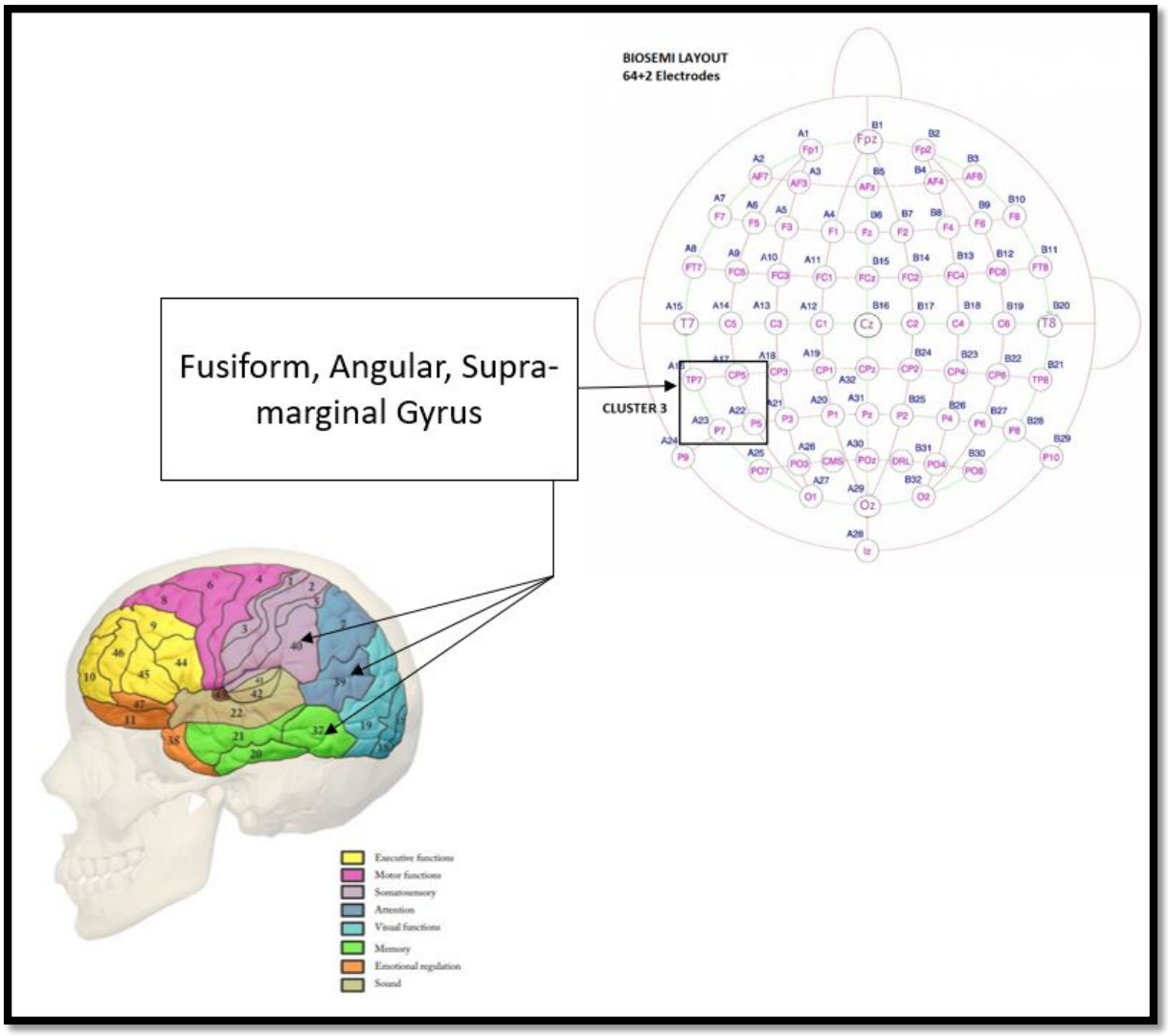

Figure 4.4: Area under Cluster 3 and its corresponding brain region in Broadmann areas. This particular cluster has some attention and memory related functions. Fusiform, Angular, Supra-marginal Gyrus areas are corresponding to this cluster, primarily located at Broadmann area 37, 39, and 40.

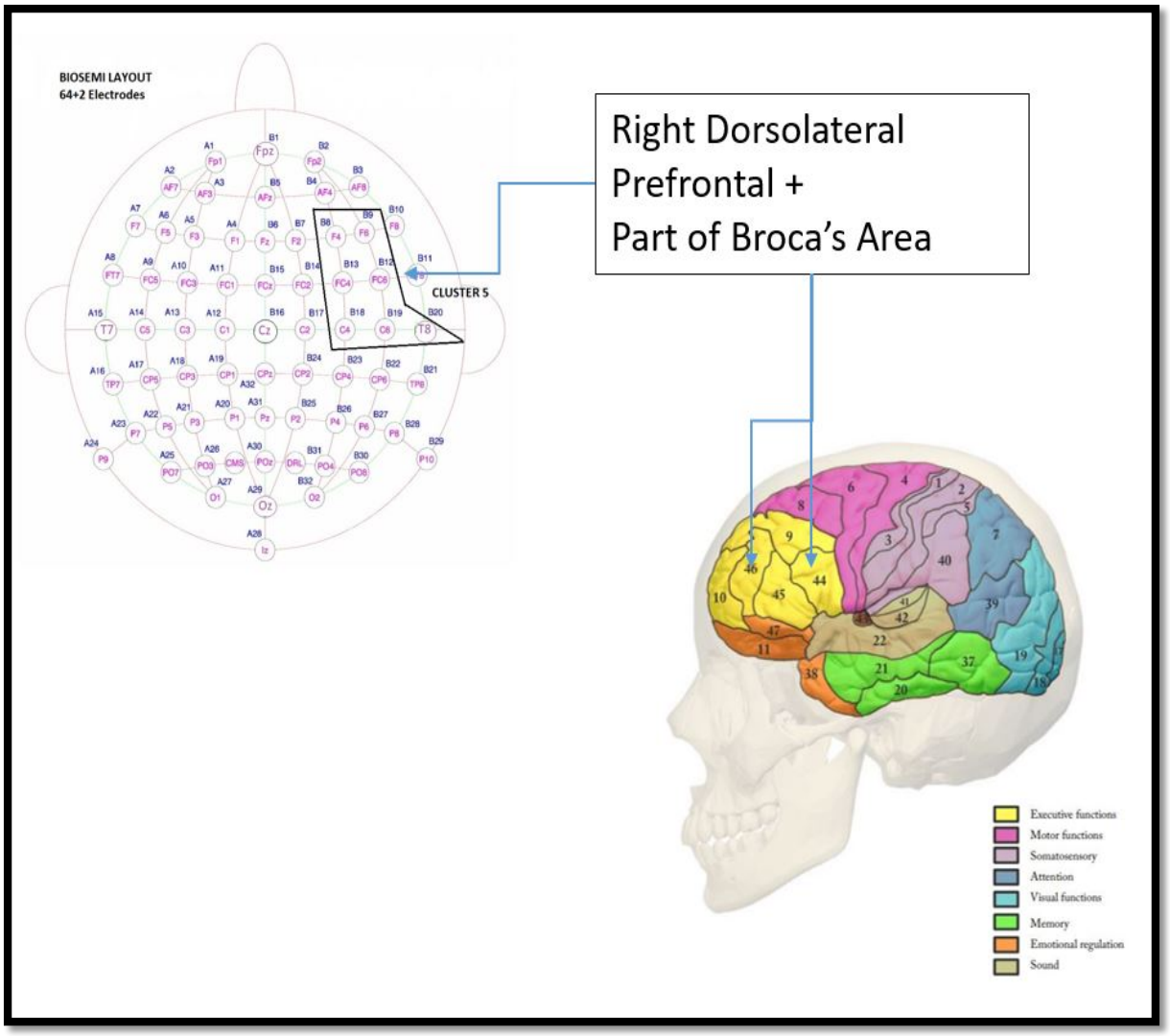

Figure 4.5: Area under Cluster 5 and its corresponding brain region in Broadmann areas. Right Dorsolateral Prefrontal and some part of Broca's areas are corresponding to this cluster, and they have some prominent executive functions in the brain.

Cluster 5 is located at right Dorsolateral Prefrontal (area 46), part of Broca's area (area 44), and some part of anterior to premotor cortex. This cluster is particularly showing significance for Delta and Beta Bands. Some common associated function of this cluster related to our study: memory retrieval (right brain), pain anticipation, expression of emotional information (right brain), and internal mental calculation [30].

In summary, this particular decision-making task involves high-level cognitive capacity along with other networks to proceed with a proper decision. Therefore, according to the electrophysiology in the brain, it is observed that there are multiple regions activated and deactivated as a response to the task. Other than these major contributions, there are multiple other areas working together to produce a well-processed response. According to our findings, dorsolateral prefrontal cortex plays the key role in decision-making process. Previous literature suggested that lateral prefrontal cortex is primarily responsible for cognitive control in terms of planning and working memory, which is similar to our findings. In a fMRI-based study, it is observed that during the goal hierarchical state the left DLPFC was significantly activated where the subjects were given the task of "Tower of London"[31]. Left Dorsolateral prefrontal(Cluster 2) is prominently activated for all three bands in our case(FDR-corrected). Moreover, the subject must execute a movement to enter the order quantity based on his/her decision in the computer keyboard, which proves of a task of the dorsolateral prefrontal cortex[32]. It is also observed that the right Dorsolateral Prefrontal and some part of Broca's area(Cluster 5) are activated for Beta band during the task which is usually tend to activate during decision making under risky conditions. These areas are suggested to be one of the significant components in the reward pathway[33]. Theta correlates memory retrieval and decision-making [28]. However, due to the

sample size, we don't see significance after statistical analysis for this band, even though theta activation was significantly observed among all clusters for decision-making.

From the physiological perspective, it is important to study decision-making phase and feedback phase with respect to the resting phase. As baseline and resting-state topoplots weren't showing much difference, each of these phases were studied compared to the baseline. Each of the task phases, Decision and Feedback, weren't showing much significance when compared to the baseline using statistical paired-t-test, even with the FDR-correction. Most number of significant electrodes are found only between two different task conditions. However, it is critical to study each of the decision-making phase compared to the immediate resting state data.

Clustering gives us an overall idea of what brain region gets involved in this complicated decision-making study and its significance. Clustering was done based on the significant electrodes found by FDR-corrected paired-t-test. However, another possible way of this clustering could be based on the regions showing significant activation/deactivation from the topoplots, and then a simple paired-t-test can be done to identify the significant clusters.

Moreover, this study consisted of 13 subjects, where the sample size is statistically low. Therefore, it is appropriate to have a large sample size to generate statistically more significant results. Further, an extended study can be useful to see if there are more interesting findings related to the performance level of the subjects.

4.2 Future Scope:

The scope of my study was to observe how brain activation take place while taking economic decisions. More subjects can be studied for improved statistical performance. Certain robust EEG algorithms can be developed based on group-level study. EEG usually suffers with localization problem due to its low spatial resolution. Group ICA and source reconstruction can be helpful to overcome this problem. Further investigations can be performed based on subject's performance level and behavioral level analysis. Moreover, different functional connectivity approaches (e.g-Dynamic Functional Connectivity) can be applied to evaluate the connectivity strengths during task performance studies [29].

CHAPTER 5

APPENDIX

5.1 Family-wise Error Rate (FWER):

In statistics, family-wise error rate (FWER) is the probability of making one or more false discoveries, or type I errors when performing multiple hypotheses tests.

The following table defines the possible outcomes when testing multiple null hypotheses. Suppose we have a number m of null hypotheses, denoted by: H_1, H_2,..., H_m. Using a statistical test, we reject the null hypothesis if the test is declared significant. We do not reject the null hypothesis if the test is non-significant. Summing each type of outcome over all Hi yields the following random variables:

	Null hypothesis is true (H_0)	Alternative hypothesis is true (H_A)	Total
Test is declared significant	V	S	R
Test is declared non-significant	U	T	$m - R$
Total	m_0	$m - m_0$	m

From the table, the parameters are defined as below:

- m is the total number hypotheses tested.
- mo is the number of true null hypotheses, an unknown parameter
- m-mo is the number of true alternative hypotheses
- V is the number of false positives (Type I error) (also called "false discoveries")

- *S* is the number of true positives (also called "true discoveries")
- *T* is the number of false negatives (Type II error)
- *U* is the number of true negatives
- R = V+S is the number of rejected null hypotheses (also called "discoveries", either true or false)

In *m* hypothesis tests of which mo are true null hypotheses, *R* is an observable random variable, and *S*, *T*, *U*, and *V* are unobservable random variables.

5.1.1 Definition:

The FWER is the probability of making at least one type I error in the family,

$$\mathrm{FWER} = \Pr(V \geq 1),$$

Thus, by assuring, $\mathrm{FWER} \leq \alpha$, the probability of making one or more type I errors in the family is controlled at level alpha.

5.1.2 Bonferroni Correction:

The Bonferroni correction is one of several methods used to counteract the problem of multiple comparisons in FWER.

If a particular test yields correct results 99% of the time, running 100 tests could lead to a false result somewhere in the mix. The Bonferroni test attempts to prevent data from incorrectly appearing to be statistically significant by lowering the alpha value.

The Bonferroni test, also known as the "Bonferroni correction" or "Bonferroni adjustment" suggests that the "p" value for each test must be equal to alpha divided by the number of tests.

For example, if a trial is testing for 20 hypothesis at desired alpha level = 0.05, then the Bonferroni correction would test each individual hypothesis at alpha =0.05/20=0.0025.

For our study, the trial is being tested for 64 hypothesis (channels), then the Bonferroni correction would test each individual hypothesis at alpha =0.05/64=0.00078.

5.2 False Discovery Rate (FDR):

The false discovery rate (FDR) is a method of conceptualizing the rate of type I errors in null hypothesis testing when conducting multiple comparisons. FDR-controlling procedures are designed to control the expected proportion of "discoveries" (rejected null hypotheses) that are false (incorrect rejections). FDR-controlling procedures provide less stringent control of Type I errors compared to familywise error rate (FWER) controlling procedures (such as the Bonferroni correction), which control the probability of at least one Type I error. Thus, FDR-controlling procedures have greater power, at the cost of increased numbers of Type I errors.

Benjamini-Hochberg procedure is very popular for compensating type I error by controlling the FDR at level alpha.

From the notation, $FDR = E(\frac{V}{R})$, The FDR is defined to be 0 if only R =0.

Suppose, we perform test on m voxels in this case. Considering the table from FWER, it will give us an overview of the voxels which are declared active, but actually inactive. So, if we didn't declare any voxel active, we can't have any false positives. The whole procedure work as follows:

- Set the desired limit at alpha on FDR(e.g., α = 0.05)
- Compute the p-value of m hypotheses

- Order them or sort them out in increasing order of p-value (e.g ranking parameter, i=1,2,3,…)
- Let r be the largest i(ranking order) such that , $p(i) \leq \frac{i}{m} * \alpha$
- Reject all hypothesis corresponding to $p(1), \ldots, p(r)$.

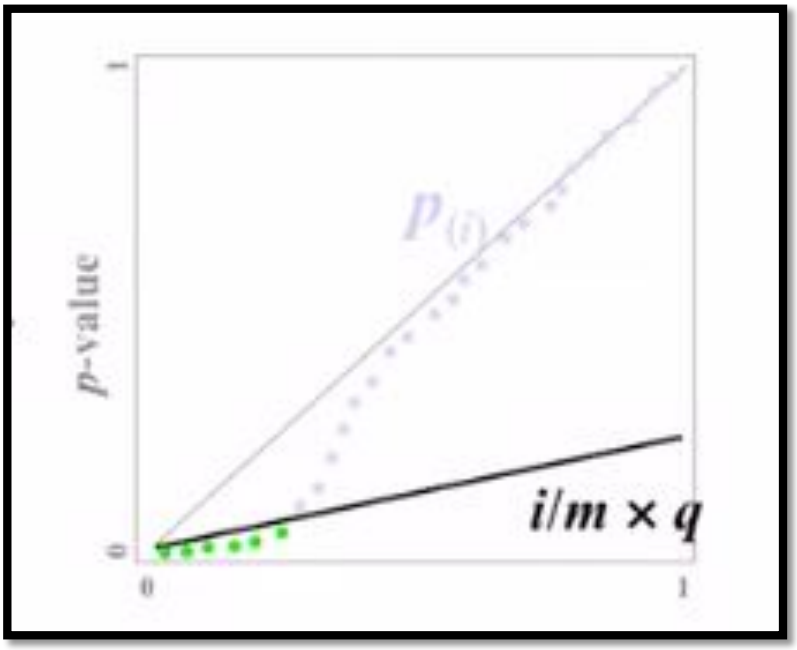

Figure 5.1: illustrates the Benjamini-Hochberg procedure for controlling the FDR at level alpha = 0.05. The black straight-line is the threshold slope, and any p-values below the threshold curve are considered as significant voxels or active voxels. Anything above the threshold are considered as inactive voxels.

If all null hypothesis are true, the FDR is equivalent to the FWER. Any procedure that controls the FWER, also controls the FDR. A procedure that controls the FDR, only can be less stringent, and lead to a gain in power. Since, FDR controlling procedures work only on the p-values, and not on the actual test statistics, it can be applied to any valid statistical tests.

In the last couple of years, FDR-controlling procedure is becoming pretty popular as they are less conservative comparing to family-wise error rate (FWER). So, they are being used a lot in neuro-imaging and big-data context recently.

In our study, we performed the Bonferroni correction between multiple hypotheses and couldn't find much significant results. However, implementing FDR-correction give us significant active electrodes for three of the bands, namely- Delta, Alpha, and Beta. All of the FDR-controlling plots are given below:

Delta:

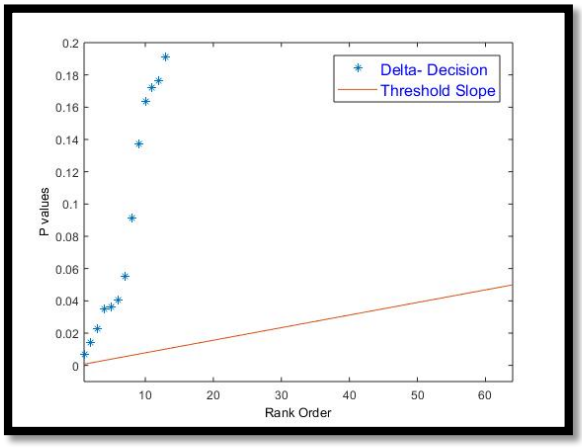

(a)

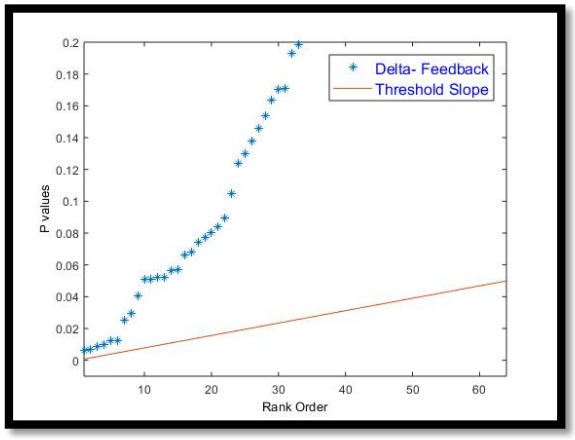

(b)

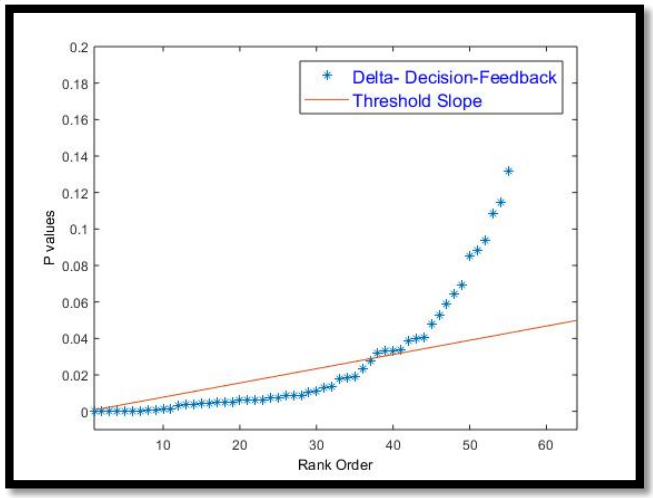

(c)

Figure 5.2: FDR-controlling plot for Delta band; (a) showing no significant p-values (corresponding electrodes) between Decision and Baseline, (b) showing no significant p-values (corresponding electrodes) between Feedback and Baseline, and (c) showing 37 significant active electrodes only during decision and feedback task.

Theta:

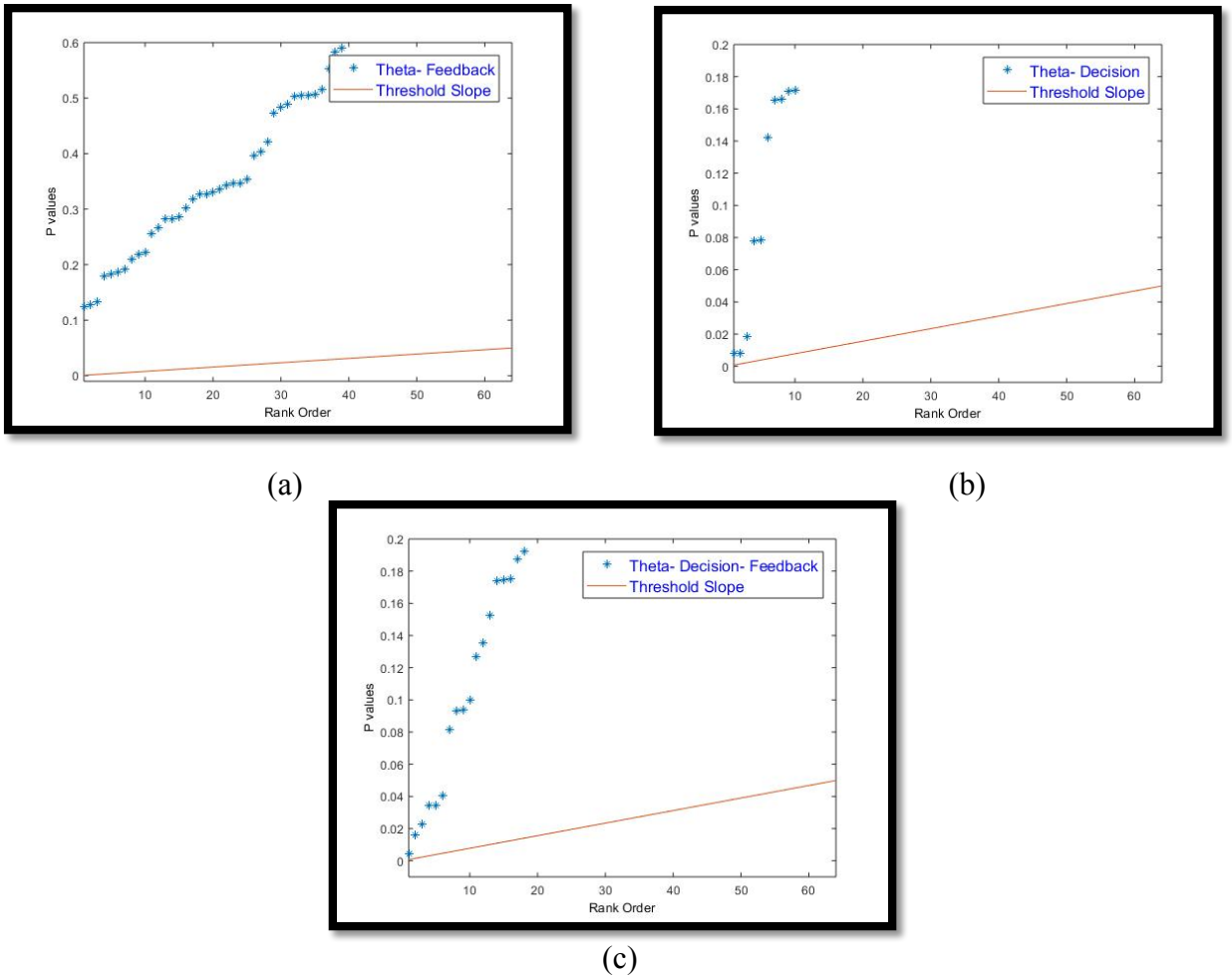

(a) (b)

(c)

Figure 5.3: FDR-controlling plot for Theta band; showing no significant active electrodes during any of the testing conditions. (a) showing no significant p-values (corresponding electrodes) between Decision and Baseline, (b) showing no significant p-values (corresponding electrodes) between Feedback and Baseline, and (c) showing no significant active electrodes during decision and feedback task.

Alpha:

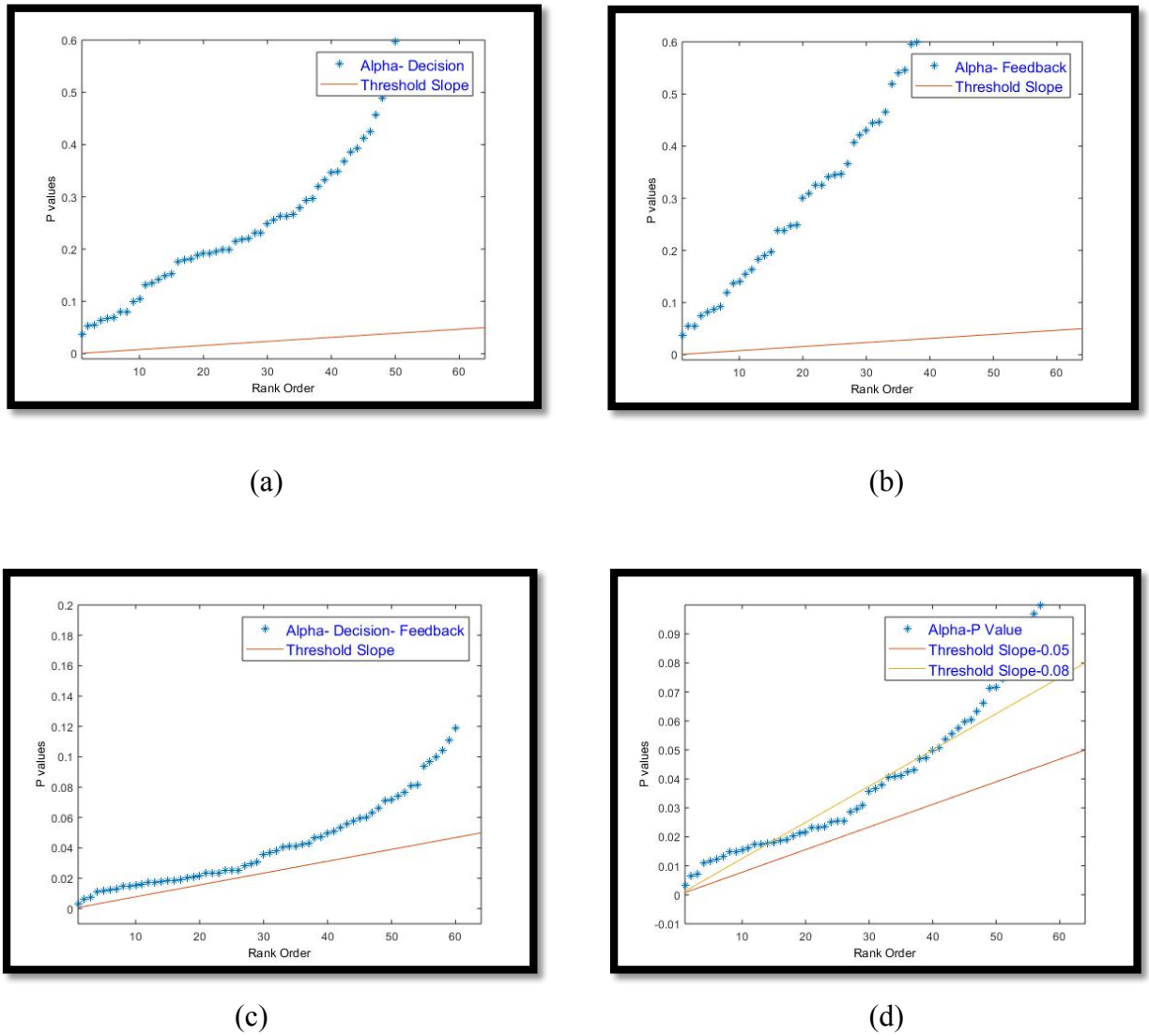

Figure 5.4: FDR-controlling plot for Alpha band, showing no significant active electrodes only during any of the testing conditions. However, increasing the threshold slope from 0.05 to 0.08, around 40 electrodes are observed as significant or true positive. (a) showing no significant p-values (corresponding electrodes) between Decision and Baseline, (b) showing no significant p-values (corresponding electrodes) between Feedback and Baseline, (c) showing no significant active electrodes during decision and feedback task, and (d) showing 40 significant electrodes after increasing the threshold slope from 0.05 to 0.08, between decision and feedback.

Beta:

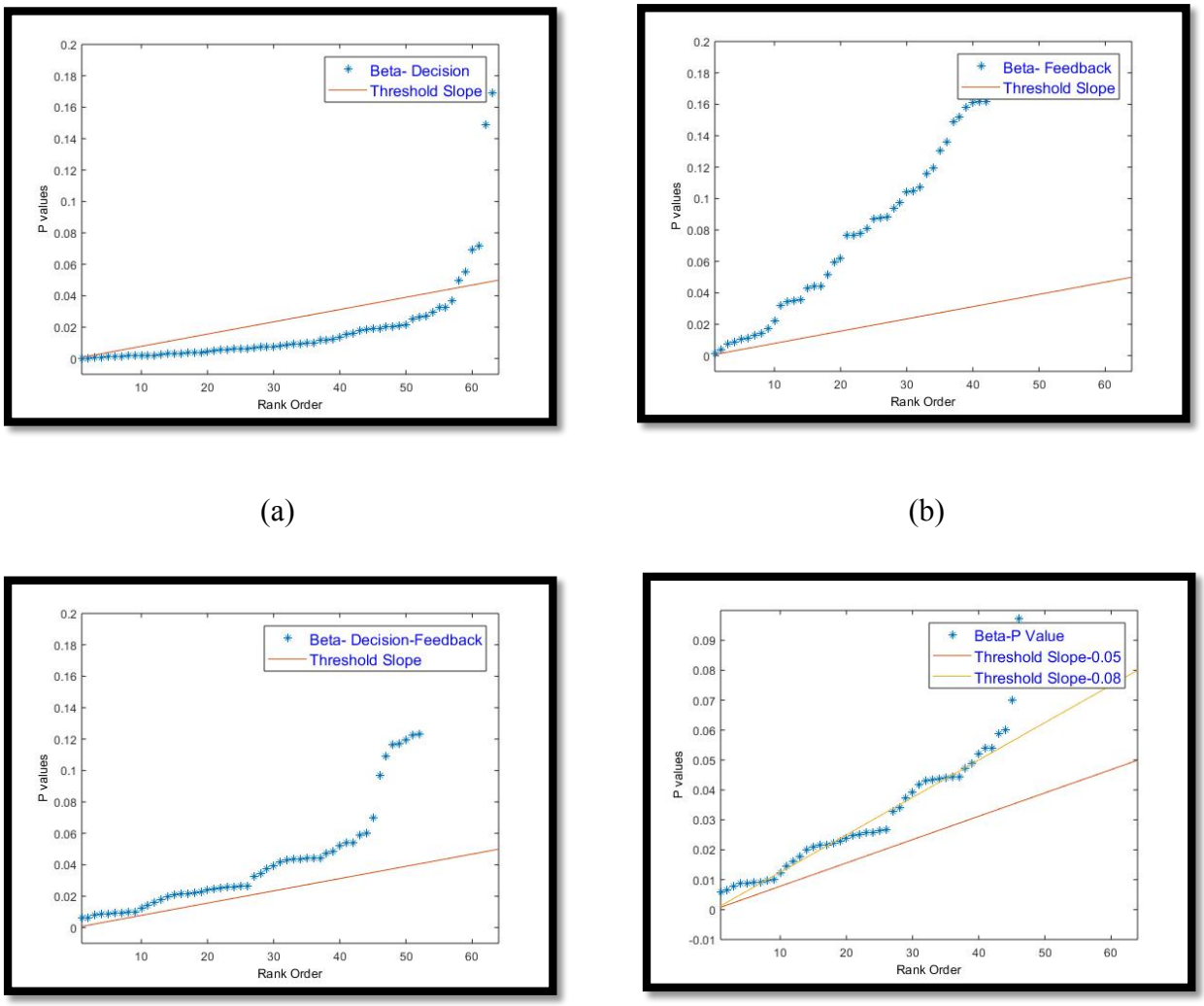

Figure 5.5: FDR-controlling plot for Beta band, showing no significant active electrodes during any of the testing conditions. However, increasing the threshold slope from 0.05 to 0.08, around 30 electrodes are observed as significant or true positive. (a) showing 58 significant p-values (corresponding electrodes) between Decision and Baseline, (b) showing no significant p-values (corresponding electrodes) between Feedback and Baseline, (c) showing no significant active electrodes during decision and feedback task, and (d) showing 30 significant electrodes after increasing the threshold slope from 0.05 to 0.08 between decision and feedback task conditions.

Gamma:

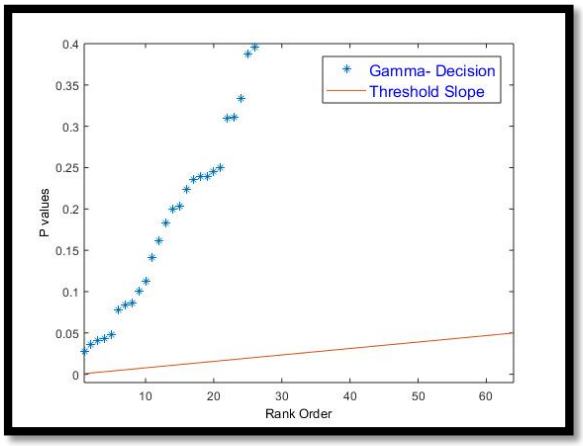

(a)

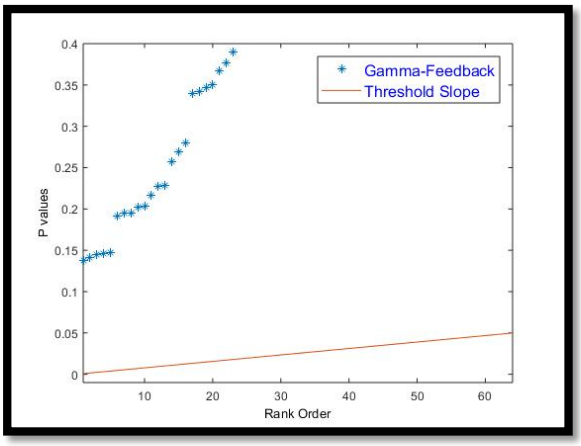

(b)

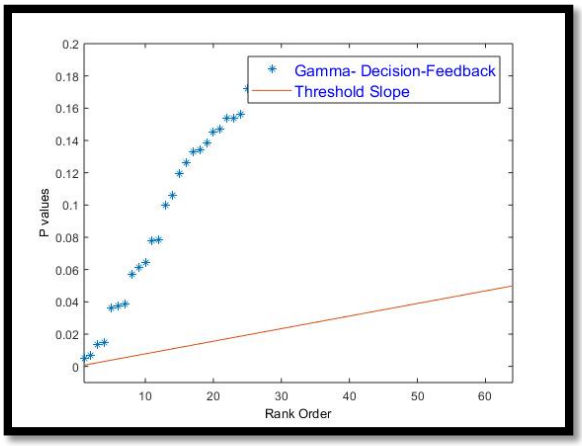

(c)

Figure 5.6: FDR-controlling plot for Gamma band; showing no significant active electrodes during any of the testing conditions. (a) showing no significant p-values (corresponding electrodes) between Decision and Baseline, (b) showing no significant p-values (corresponding electrodes) between Feedback and Baseline, and (c) showing no significant active electrodes during decision and feedback task.

Power Comparison: Theta Band

Observation:

From the figure 5.7, it is observed that Theta band is showing significant activation for all five clusters for decision-making phase. On the other hand, feedback is showing quite the opposite nature, significant deactivation for four clusters, other than cluster 1. Previous studies reported that Theta plays a key role in memory retrieval and decision-making.[28] Our findings suggest that Theta has significant activation for all five clusters during decision-making phase. All the error bars are based on the standard error of the mean in all comparisons. Cluster 2 and 3 are showing statistically significance among decision and feedback phase. Each of these clusters have meaningful working functions in the brain.

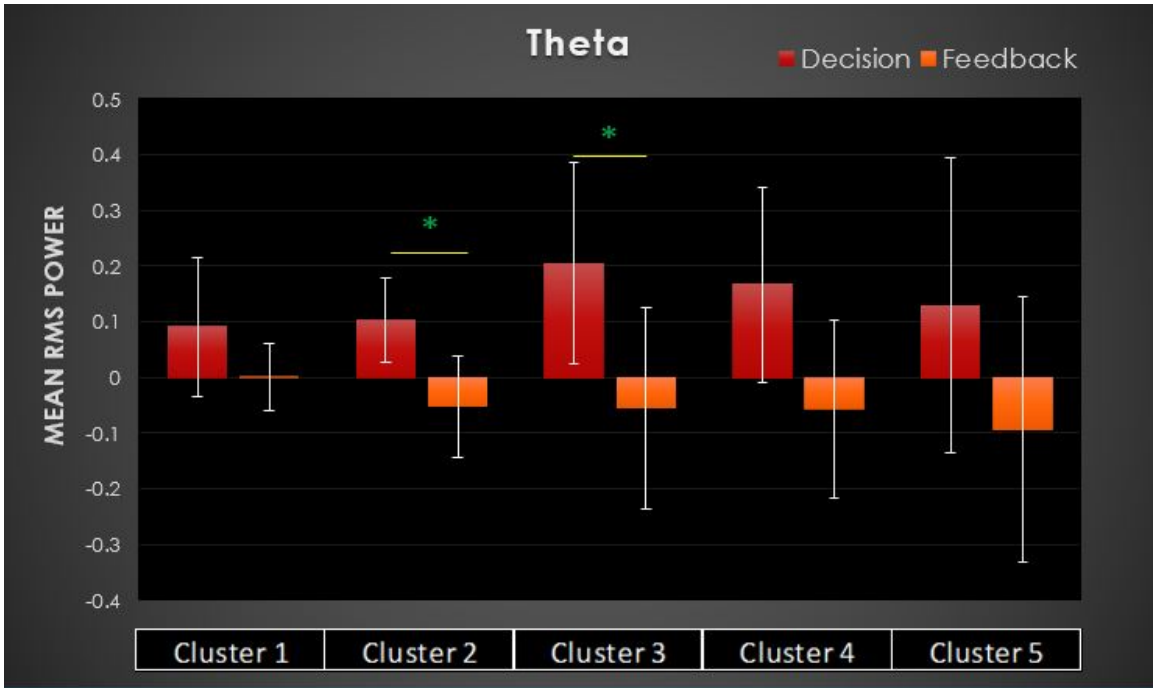

Figure 5.7: Mean RMS power comparison of Decision-making and Feedback Phase for five clusters for Theta band. The error bar is based on the standard error of the mean, and the '' represents the significance under FDR correction for decision-making and feedback phase for two clusters.*

Discussion:

Studies consistently report frontal theta activity to correlate with the difficulty of mental operations, for example during focused attention and information uptake, processing and learning or during memory recall. Theta frequencies become more prominent with increasing task difficulty. This is why theta is generally associated with brain processes underlying mental workload or working memory [10]. (Klimesch, 1996; O'Keefe & Burgess, 1999; Schack, Klimesch, & Sauseng, 2005).

Power Comparison: Gamma Band

Observation:

From the figure 5.8, it can be stated that gamma band is usually showing deactivation during decision-making phase. On the other hand, this high-frequency component is showing some activation during feedback phase for cluster 4 and cluster 5. Only one of the clusters are significantly showing difference between decision-making and feedback task conditions.

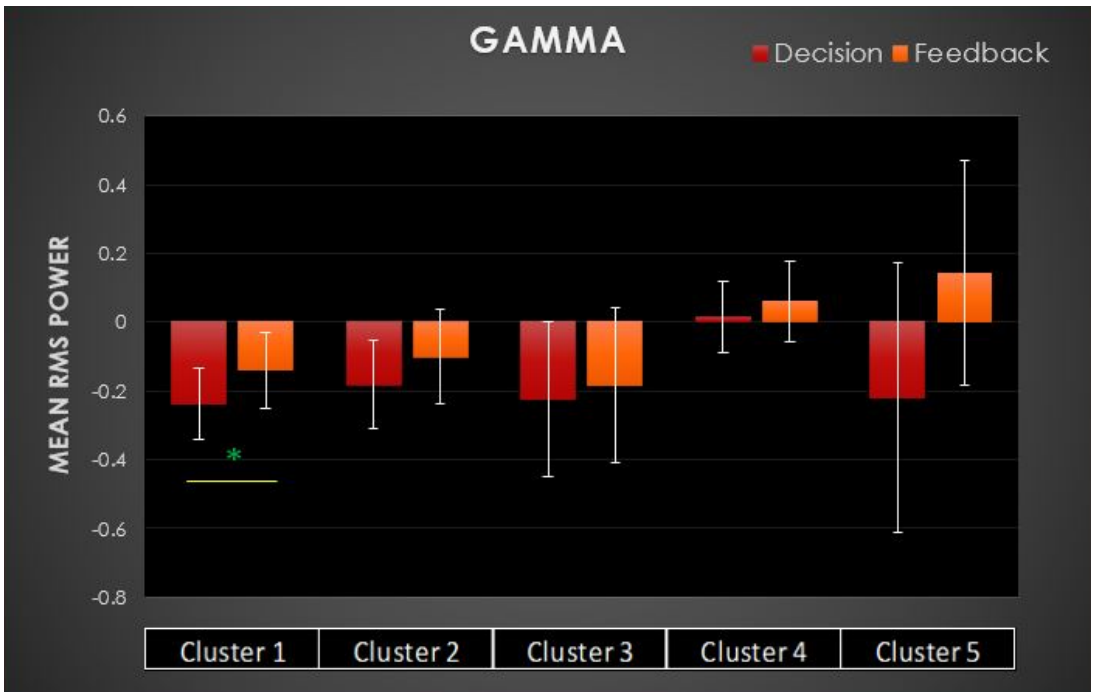

Figure 5.8: Mean RMS power comparison of Decision-making and Feedback Phase for five clusters for Gamma band. The error bar is based on the standard error of the mean, and the '' represents the significance under FDR correction for decision-making and feedback phase for one cluster.*

Discussion:

From the characteristic of Gamma, Gamma is usually more prominent in stress, anxiety or high arousal condition. Gamma band shows some significant activation in right dorsolateral prefrontal cortex, which is primarily responsible for internal mental calculation and working memory. Thus, activation in feedback phase for this high frequency component can be due to high stress in low-margin treatment condition.

REFERENCES

[1] Ayse Kocalbiyikoglu, Celile Itir Gogus et el(2015), 'Decision Making and the Price Setting Newsvendor: Experimental Evidence'

[2] U. Benzion, Y. Cohen, R. Peled, and T. Shavit, "Decision-making and the newsvendor problem: an experimental study," *J. Oper. Res. Soc.*, vol. 59, no. 9, pp. 1281–1287, Sep. 2008.

[3] H. Gaspars-Wieloch, "Newsvendor problem under complete uncertainty: a case of innovative products," *Cent. Eur. J. Oper. Res.*, vol. 25, no. 3, pp. 561–585, Sep. 2017.

[4] A. L. Krain, A. M. Wilson, R. Arbuckle, F. X. Castellanos, and M. P. Milham, "Distinct neural mechanisms of risk and ambiguity: A meta-analysis of decision-making," *NeuroImage*, vol. 32, no. 1, pp. 477–484, Aug. 2006.

[5] M. E. Schweitzer and G. P. Cachon, "Decision Bias in the Newsvendor Problem with a Known Demand Distribution: Experimental Evidence," *Manag. Sci.*, vol. 46, no. 3, pp. 404–420, Mar. 2000.

[6] D. C. Farrar, A. Z. Mian, A. E. Budson, M. B. Moss, and R. J. Killiany, "Functional brain networks involved in decision-making under certain and uncertain conditions," *Neuroradiology*, vol. 60, no. 1, pp. 61–69, Jan. 2018. –motivation by fMRI studies

[7] Yajing Si, Xi Wu, Fali Li (Dec 2018)- Why EEG over other modalities?

[8] Bryn Farnsworth(2018), "What is EEG (Electroencephalography) and How Does it Work? "

https://imotions.com/blog/what-is-eeg/

[9] Harmony, T. (2013). 'The functional significance of delta oscillations in cognitive processing.' Frontiers in Integrative Neuroscience.7:83 10.3389/fnint.2013.00083

[10] Klimesch, W. (1999). EEG alpha and theta oscillations reflect cognitive and memory performance: a review and analysis. Brain Res. Rev., 29 (2-3), 169–195

[11] Craig, A., Tran, Y., Wijesuriya, N., Nguyen, H. (2012). Regional brain wave activity changes associated with fatigue. Psychophysiology 49:574–582

[12] Klimesch, W. (2012). Alpha-band oscilaltions, attention, and controlled access to stored information. Trends Cogn Sci.16(12):606–17. 10.1016/j.tics.2012.10.007

[13] Takahashi, K., Saleh, M., Penn, R. D., Hatsopoulos, N. G. (2011). Propagating waves in human motor cortex. Front Hum Neurosci. 5(40):40

[14] Halder, S., Agorastos, D., Veit, R., Hammer, E. M., Lee, S., Varkuti, B., et al. (2011). Neural mechanisms of brain-computer interface control. Neuroimage 55, 1779–1790. Doi: 10.1016/j.neuroimage.2011.01.021

[15] Jia, X., Kohn, A. (2011). Gamma Rhythms in the Brain. PLOS Biology. 9(4):e1001045 doi: 10.1371/journal.pbio.1001045

[16] Yuval-Greenberg, S., Tomer, O., Keren, A. S., Nelken, I., Deouell, L. Y. (2008). Transient induced gamma-band response in EEG as a manifestation of miniature saccades. Neuron. 58: 429–41. doi: 10.1016/j.neuron.2008.03.027

[17] iMotions(2016), 'EEG(Electroencephalography): The Complete Pocket Guide'

https://imotions.com/blog/eeg/

[18] Ali A.Abdul-latif, Irena Cosic, Dinesh K.Kumar, Barbara Polus et el(2004), 'Power changes of EEG signals associated with muscle fatigue: The Root Mean Square analysis of EEG bands', IEEE Transaction

[19] Hindarto, Moh. Hariadi, Mauridhi Hery Purnomo et el.(2014), 'EEG SIGNAL IDENTIFICATION BASED ON ROOT MEAN SQUARE AND AVERAGE POWER SPECTRUM BY USING BACKPROPAGATION', Journal of Theoretical & Applied Information Technology

[20] A. Delorme, T. Mullen, C. Kothe, Z. Akalin Acar, N. Bigdely-Shamlo, A. Vankov*, et al.*, "EEGLAB, SIFT, NFT, BCILAB, and ERICA: new tools for advanced EEG processing," *Comput Intell Neurosci,* vol. 2011, p. 130714, 2011. –EEGLAB

[21] Tzyy-Ping Jung, Scott Makeig, Colin Humphries, Te-Won Lee, Martin J. Mckeown, Vicente Iragui*, et al.*, "Removing electroencephalographic artifacts by blind source seperation," *Psychophysiology,* vol. 37, pp. 163-178, 2000. – removing artifacts

[22] Re-referencing: *Hagemann D, Naumann E, Thayer JF, '*The quest for the EEG reference revisited: a glance from brain asymmetry research.' *Psychophysiology. 2001 Sep; 38(5):847-57.*

[23] Verónica Nácher, Anders Ledberg, Gustavo Deco, Ranulfo Romo, 'Coherent delta-band oscillations between cortical areas correlate with decision making', Neuroscience v.110, September 2013

[24] Zachary Yaple, Mario Martinez-Saito, Nikita Novikov et al.(2018), 'Power of Feedback-Induced Beta Oscillations Reflect Omission of Rewards: Evidence From an EEG Gambling Study' *Frontier Neuroscience, vol 12 ,2018*

[25] F.H Duffy, 'Topographic Mapping of Brain Electrical Activity: Clinical Applications and Issues', Topographic Brain Mapping of EEG and Evoked Potentials, pp 19-52

[26] A. Widmann, E. Schroger, and B. Maess, "Digital filter design for electrophysiological data--a practical approach," *J Neurosci Methods,* vol. 250, pp. 34-46, Jul 30 2015.
[27] T. Mullen, "NITRC: CleanLine: Tool/Resource Info.," 2012.

[28] Jacobs J, Hwang G, Curran T, Kahana MJ et. el (2006), 'EEG oscillations and recognition memory: theta correlates of memory retrieval and decision making.', Neuroimage 2006 Aug 15;32(2):978-87.

[29] Angus Ho Ching Fong, Kwangsun Yoo, Monica D. Rosenberg, 'Dynamic functional connectivity during task performance and rest predicts individual differences in attention across studies', NeuroImage(March 2019)

[30] Cortical Functions- Trans Cranial Technologies(2012)

[31] C. P. Kaller, B. Rahm, J. Spreer, C. Weiller, and J. M. Unterrainer, "Dissociable contributions of left and right dorsolateral prefrontal cortex in planning," *Cereb. Cortex N. Y. N 1991*, vol. 21, no. 2, pp. 307–317, Feb. 2011.

[32] E. Hoshi and J. Tanji, "Area-Selective Neuronal Activity in the Dorsolateral Prefrontal Cortex for Information Retrieval and Action Planning," *J. Neurophysiol.*, vol. 91, no. 6, pp. 2707–2722, Jun. 2004.

[33] K. I. Bolla *et al.*, "Orbitofrontal cortex dysfunction in abstinent cocaine abusers performing a decision-making task," *NeuroImage*, vol. 19, no. 3, pp. 1085–1094, Jul. 2003.

[34] Juti Naraballobh, Dusit Thanapatay, Jatuporn Chinrungrueng, 'Effect of auditory stimulus in EEG signal using a Brain-Computer Interface', IEEE Explore, August 2015.

[35] Richard A. Armstrong et. El(2014), 'When to use the Bonferroni Correction', Ophthalmic & Physiological Optics, vol 34, issue 5.

[36] Archana K. Singh, Hideki Asoh, Yuji Takeda, Steven Phillips, 'Statistical Detection of EEG Synchrony Using Empirical Bayesian Inference', PLoS One, v.10(3), March 2015

[37] Davis CE, Hauf JD, Wu DQ, Everhart DE, 'Brain function with complex decision making using electroencephalography.' Int J Psychophysiology 2011 Feb;79(2):175-83.

[38] Nabila Salma, Bin Mai, Kamesh Namuduri et. el(2017), 'Using EEG Signal to Analyze IS Decision Making Cognitive Processes', Information Systems and Neuroscience, pp 211-218